The electron-bifurcating FeFe-hydrogenase Hnd is involved in ethanol metabolism in Desulfovibrio fructosovorans grown on pyruvate

Natalie Payne, Arlette Kpebe, Chloé Guendon, Carole Baffert, Julien Ros, Régine Lebrun, Yann Denis, Laetitia Shintu, Myriam Brugna

The electron-bifurcating FeFe-hydrogenase Hnd is involved in ethanol metabolism in *Desulfovibrio fructosovorans* grown on pyruvate

Natalie Payne[+1], Arlette Kpebe[+1], Chloé Guendon[1], Carole Baffert[1], Julien Ros[1], Régine Lebrun[2], Yann Denis[3], Laetitia Shintu[4] and Myriam Brugna[1]*

[1]CNRS, Aix Marseille Univ, BIP, Marseille, France

[2]CNRS, Aix Marseille Univ, Plate-forme Protéomique de l'IMM, FR 3479, Marseille Protéomique (MaP), Marseille, France

[3]CNRS, Aix Marseille Univ, Plate-forme Transcriptomique, Marseille, France

[4]CNRS, Aix Marseille Univ, Centrale Marseille, ISM2, Marseille, France

Co-author email adresses: Natalie Payne: npayne@imm.cnrs.fr; Arlette Kpebe: akpebe@imm.cnrs.fr; Chloé Guendon: cguendon@imm.cnrs.fr; Carole Baffert; cbaffert@imm.cnrs.fr; Julien Ros: julienros@laposte.net; Régine Lebrun: rlebrun@imm.cnrs.fr; Yann Denis; ydenis@imm.cnrs.fr; Laetitia Shintu: laetitia.shintu@univ-amu.fr; Myriam Brugna: mbrugna@imm.cnrs.fr

[+]N. Payne and A. Kpebe should be considered joint first author

*Corresponding author: Myriam Brugna, Laboratoire de Bioénergétique et Ingénierie des Protéines, CNRS, 31 Chemin Joseph Aiguier, 13402, Marseille Cedex 20, France. mbrugna@imm.cnrs.fr

+33 4 91 16 45 68

Orcid ID Myriam Brugna: 0000-0002-4017-3294

Running title: Role of the electron-bifurcating hydrogenase Hnd

Keywords: Hydrogenase, Electron bifurcation, *Desulfovibrio*, Alcohol dehydrogenase, Aldehyde ferredoxin oxidoreductase, Ethanol

Abstract

Desulfovibrio fructosovorans, a sulfate-reducing bacterium, possesses six gene clusters encoding six hydrogenases catalyzing the reversible oxidation of H_2 into protons and electrons. Among them, Hnd is an electron-bifurcating hydrogenase, coupling the exergonic reduction of NAD^+ to the endergonic reduction of a ferredoxin with electrons derived from H_2. It was previously hypothesized that its biological function involves the production of NADPH necessary for biosynthetic purposes. However, it was subsequently demonstrated that Hnd is instead a NAD^+-reducing enzyme, thus its specific function has yet to be established. To understand the physiological role of Hnd in *D. fructosovorans*, we compared the *hnd* deletion mutant with the wild-type strain grown on pyruvate. Growth, metabolites production and comsumption, and gene expression were compared under three different growth conditions. Our results indicate that *hnd* is strongly regulated at the transcriptional level and that its deletion has a drastic effect on the expression of genes for two enzymes, an aldehyde ferredoxin oxidoreductase and an alcohol dehydrogenase. We demonstrated here that Hnd is involved in ethanol metabolism when bacteria grow fermentatively and proposed that Hnd might oxidize part of the H_2 produced during fermentation generating both NADH and reduced ferredoxin for ethanol production via its electron bifurcation mechanism.

Introduction

Sulfate reducers belonging to the δ-Proteobacterial genus *Desulfovibrio* are ubiquitous in anoxic habitats and employ a respiratory metabolism with sulfate as the terminal electron acceptor. Molecular hydrogen plays an important role in the energy metabolism of these bacteria which can switch from respiration to fermentation. Depending on the growth conditions, H_2 can be used as the sole energy source during respiration or produced in order to oxidize reduced electron carriers to maintain the continuous conversion of the substrates during fermentation (Thauer *et al.*, 2007, Fauque *et al.*, 1988, Rabus *et al.*, 2013). This ability of *Desulfovibrio* to consume and produce hydrogen is exploited during syntrophic associations anaerobic environments (Bryant *et al.*, 1977, Stolyar *et al.*, 2007, Meyer *et al.*, 2013a, Meyer *et al.*, 2013b).

Hydrogenases, the key enzymes involved in the metabolism of molecular hydrogen, catalyze the reversible oxidation of H_2 into protons and electrons. Most of the known hydrogenases are iron-sulfur proteins and are classified into two main distinct families according to the two metal atoms at their active site, the [NiFe]-hydrogenases (Volbeda *et al.*, 1995, Higuchi *et al.*, 1997) and the [FeFe]-hydrogenases (Peters *et al.*, 1998, Nicolet *et al.*, 1999). These enzymes are widely distributed in *Bacteria* and *Archaea* as well as in unicellular eukaryotes (Vignais *et al.*, 2001, Vignais & Billoud, 2007, Benoit *et al.*, 2020).

The versatility of the *Desulfovibrio* H_2 metabolism is due to a complex hydrogenase system composed of several different enzymes located in different cellular compartments (Thauer *et al.*, 2007, Pereira *et al.*, 2011, Baffert *et al.*, 2019). The number, the type and the cellular location of these enzymes vary considerably from one *Desulfovibrio* species to another (Pereira *et al.*, 2011, Baffert *et al.*, 2019) and this diversity makes the role of these various hydrogenases difficult to determine. Forty years ago, a model for the growth of *Desulfovibrio* in lactate medium in the presence of sulfate, the “hydrogen cycling model”, was proposed (Odom & Peck, 1981). In this model, electrons and protons produced by lactate oxidation are used by a cytoplasmic hydrogenase to produce H_2. After the diffusion through the cytoplasmic membrane, H_2 is re-oxidized by a periplasmic hydrogenase contributing to the proton gradient across the membrane used for ATP synthesis. The electrons generated by this oxidation are then returned to the cytoplasm through several integral membrane complexes where they are used for sulfate reduction. Since then, several models for energy conservation in

Desulfovibrio have been proposed in which, in addition to the H_2 recycling pathway, there is another H_2-independent pathway involving a direct electron transfer from the donor to the acceptor (Keller & Wall, 2011, Noguera *et al.*, 1998, Sim *et al.*, 2013).

In *Desulfovibrio fructosovorans*, our biological model, three hydrogenases have been already characterized: Hyn, a periplasmic [NiFe]-hydrogenase (Hatchikian *et al.*, 1990, Rousset *et al.*, 1990); Hyd, a periplasmic [FeFe]-hydrogenase (Casalot *et al.*, 1998) and Hnd, a cytoplasmic [FeFe]-hydrogenase (Malki *et al.*, 1995, de Luca *et al.*, 1998, Kpebe *et al.*, 2018). *D. fructosovorans* genome analysis revealed the presence of three genes clusters encoding three additional putative hydrogenases (Baffert *et al.*, 2019): a membrane-bound Ech-type hydrogenase, a cytoplasmic trimeric [FeFe]-hydrogenase Hnt similar to the electron-bifurcating hydrogenase from *Thermotoga maritima* (Schut & Adams, 2009), and a [FeFe] cytoplasmic hydrogenase showing similarity with the putative sensory [FeFe]-hydrogenase HydS from *T. maritima* (Chongdar *et al.*, 2018) or the Hfs hydrogenase from *Thermoanaerobacterium saccharolyticum* (Shaw *et al.*, 2009). The specific function of these six enzymes is not yet clearly established in *D. fructosovorans*. Marker-exchange mutagenesis was performed to determine the role of hydrogenases in the energy metabolism of the bacterium (Malki *et al.*, 1997, Casalot *et al.*, 2002a, Casalot *et al.*, 2002b). Results clearly indicated an effect of the depletion of hydrogenases on the growth behavior of *D. fructosovorans*. However, it was difficult to hypothesize on the physiological implications of each hydrogenase due to enzymatic compensation processes as the result of the deletion of the genes encoding one, two or three hydrogenases (Malki *et al.*, 1997, Casalot *et al.*, 2002a, Casalot *et al.*, 2002b, Rousset *et al.*, 1991).

We recently produced and purified a recombinant form of Hnd and showed that it is an electron-bifurcating hydrogenase that simultaneously reduces two different electron acceptors, NAD^+ and a ferredoxin in the presence of H_2 (Kpebe *et al.*, 2018), despite it being previously described as an $NADP^+$-reducing enzyme (Malki *et al.*, 1995, de Luca *et al.*, 1998). Flavin-based electron bifurcation is an important mechanism of energy conservation, mainly found in anaerobic microorganisms, coupling an endergonic redox reaction to an exergonic redox reaction (Buckel & Thauer, 2018a, Buckel & Thauer, 2018b). This tetrameric enzyme is encoded by the *hnd* operon, in which *hndA* and *hndC* encode the NAD-dependent unit

and *hndD* encodes the [FeFe]-hydrogenase subunit, which is closely related to the hydrogenase CpI from *Clostridium pasteurianum* (Malki *et al.*, 1995). The function of the product of the *hndB* gene is unknown. This cytoplasmic Hnd complex catalyzes, *in vitro*, the coupled endergonic reduction of ferredoxin and the exergonic reduction of NAD^+ by the oxidation of H_2 (Kpebe *et al.*, 2018).

Initially, it was hypothesized that the biological function of Hnd involves the production of NADPH necessary for biosynthetic purposes (de Luca *et al.*, 1998) but because it was subsequently determined that Hnd is in fact a NAD^+-reducing enzyme (Kpebe *et al.*, 2018), its specific function has yet to be established. In order to understand the involvement of the electron-bifurcating Hnd hydrogenase in the energy-generating metabolism in *D. fructosovorans*, we compared the *hndD* deletion mutant strain (SM4) (Malki *et al.*, 1997) with the wild-type strain grown on different pyruvate-containing media. Our results indicate that Hnd is not essential for the bacterial growth when pyruvate is used as the carbon source, and that this hydrogenase is involved in ethanol metabolism when bacteria grow fermentatively.

Results

Growth of D. fructosovorans on pyruvate-containing media

The growth of the wild-type strain and the SM4 strain, in which the *hndD* gene encoding the hydrogenase catalytic subunit of Hnd is deleted (Malki *et al.*, 1997) was measured in batch cultures (Figure 1). Two different growth conditions were compared, both containing 25 mM pyruvate as the only source of energy: a medium containing 20 mM sulfate as electron acceptor (PS20 medium, respiratory condition) and a medium without any electron acceptor (PS0 medium, fermentative condition). Since growth during fermentation is very slow compared to sulfate respiration, the cells were also grown under a third condition in which they grow faster on a medium that contains a limiting concentration of sulfate (PS2 medium containing 2mM sulfate, mixed culture condition). In each condition, there were no striking differences among the growth curves of the two strains (Figure 1). However, growth yields as well as doubling times of both strains are significantly different under the three conditions (Table 1). In the fermentative condition,

the growth is slow for both strains but even slower for the mutant strain, with a doubling time of 369 h for the WT compared to 519,5 h for the mutant. However, the overall growth yield of the mutant is unaffected, because a similar maximum absorbance around 0.70 at 600 nm is reached for the two strains that correspond to 6.7/6.9. 10^9 cells/mL. In the respiratory condition (PS20), the growth is faster and both strains behave similarly: the growth reaches a maximum absorbance of 1.3-1.4 at 600 nm (1.33-1.41. 10^9 cells/mL) and the generation time is around 20 h for the WT strain and 15h for SM4. Under sulfate-limited conditions, the growth exhibits two different phases, a rapid one (phase 1, until around 40 h) before the sulfate is exhausted (see Figure S1 for the quantification of sulfate) and a slow one (phase 2, from around 40 h to 110 h) in which there is no more sulfate in the medium. While the generation times of phase 1 measured for both strains are similar to those of the respiratory condition, those of phase 2 are much faster than that of the fermentation condition and in this phase, the growth of the mutant strain is slightly slower than that of the WT strain. Taken together, these results indicate that Hnd is not essential for bacterial growth under either fermentative or respiratory conditions when pyruvate is used as the carbon source and that in the SM4 mutant, the generation time is affected only when there is no sulfate in the medium (fermentative condition or phase 2 of the mixed condition). On the other hand, biomass yields (maximum cell counts/mL) are not affected at all in the mutant regardless of the growth conditions.

Impact of hnd deletion on metabolite production and consumption

To evaluate the impact of *hndD* deletion on *D. fructosovorans* physiology, we compared pyruvate consumption as well as acetate, ethanol and H_2 production (Figure 2). The pyruvate is completely consumed, with the rate depending on the initial sulfate concentration in the medium: the more sulfate there is, the faster the consumption. Pyruvate consumption and acetate production are not significantly different between the two strains on PS20 and PS2 media whereas, in the absence of sulfate, both pyruvate and acetate are respectively consumed or produced slowly by the mutant than by the WT strain. However, there is a striking difference between the two strains in terms of the production of ethanol (Figure 2). Both strains produce ethanol only during mixed and fermentation conditions. In both conditions, the mutation

146 significantly affects the ethanol formation, since the SM4 mutant produces less ethanol than the WT strain
147 (4 times less in fermentation condition and 10 times less in mixed growth condition). The highest level of
148 produced ethanol is reached under fermentation conditions for both strains.

149 There is also a notable difference in H_2 production between the two strains (Figure 2). There is no
150 H_2 production in respiratory conditions for either strain. Under fermentation conditions, however, H_2
151 production is more than twice as high in the mutant as in the WT strain. Under mixed conditions, the
152 amount of H_2 in the headspace at the end of the exponential phase is 1.5 times higher for SM4 than for the
153 WT strain. However, the H_2 amount at the end of the growth is identical for both strains due to differences
154 of production kinetics. Collectively, these results show that the SM4 mutant strain is affected under mixed
155 and fermentation conditions but not under respiratory conditions, suggesting that Hnd has a role in
156 fermentative metabolism. Under fermentative conditions, the mutant produces more H_2 and less ethanol
157 than the WT strain, indicating that H_2 and ethanol production pathways are therefore affected in the
158 mutant. In this study, all subsequent analyses were performed on strains grown under respiration and
159 mixed conditions because under fermentation conditions, growth is very slow and very little cellular
160 material is obtained.

161

162 *Impact of hnd deletion at the protein level*

163 Coomassie-blue-stained SDS-PAGE was used to compare the soluble protein pattern of the WT and
164 SM4 strains grown under mixed or respiratory conditions. At the end of the exponential phase of growth,
165 total soluble proteins were prepared and migrated on SDS-PAGE (Figure 3A). The bands indicating
166 significant differences in protein levels between the two strains were cut out from the gel and the proteins
167 were identified by mass spectrometry (Figure 3B and Table S1 for complete list of identified proteins). As
168 shown in Figure 3, the protein profiles are different for the two strains. Three bands (1, 2 and 3) that were
169 significantly more intense in the WT strain than in the mutant strain were analyzed. Results are reported in
170 Figure 3B in which only proteins identified with the highest score in each gel band are reported (for a

complete list of identified proteins, see Table S1). The most striking difference concerns band 1 corresponding to a protein whose gene has been annotated as iron-containing alcohol dehydrogenase (Adh) (locus tag: DesfrDRAFT_3929). The intensity of this band suggests that this protein is very strongly produced in the WT strain whereas it is almost absent in the mutant strain under both growth conditions. Similarly, the analysis of band 3 (Figure 3) reveals the presence of a protein whose gene is annotated as aldehyde ferredoxin oxidase (Aor) (locus tag: DesfrDRAFT_2487). Band 2 (Figure 3) corresponds to the HndC subunit of Hnd. The intensities of the Adh and Aor bands in Figure 3 suggest that the amount of these two enzymes is greater in the WT strain grown in PS2 medium than in PS20.

Expression of hnd on pyruvate medium

Metabolite production analysis suggests that Hnd has a role in fermentative metabolism. Expression of *hndD* was determined in the WT strain using RT-qPCR under both mixed and respiratory conditions. Figure 4 shows that *hndD* expression is much higher (by a factor of 80) in cells grown in PS2 than in PS20. Hnd production was followed by western blot (Figure 5A). While the enzyme is detected in bacteria that grew under mixed conditions (PS2), it is not detected in those that grew in respiration condition (PS20). The same profile of Hnd production is obtained when *D. fructosovorans* used a limiting concentration of fumarate or sodium thiosulfate as electron acceptor instead of sulfate (Figure S2).

Cytoplasmic extracts of the WT strain at the early stationary phase grown in PS2 or PS20 medium were migrated on a Blue-Native gel electrophoresis followed by in-gel detection of hydrogenase activity (Figure 5B). An activity band, corresponding to Hnd (Kpebe *et al.*, 2018), is visible when the strain grew under mixed condition but not under respiratory condition, which is consistent with the higher *hndD* gene expression and the higher protein production under mixed condition than under respiration. Taken together, these results demonstrate that the expression of *hnd* operon is not constitutive and is strongly regulated at the transcriptional level, and that *hnd* expression is much higher under mixed condition than respiratory condition suggesting that the enzyme has a role in fermentative metabolism.

196

197 *aor and adh gene expression*

198 The expression of *adh* and *aor* genes was analyzed by RT-qPCR to determine if the difference in the
199 amount of the two enzymes in both strains was due to a difference in their gene expression (Figure 4). In
200 the WT strain, as for the *hnd* gene, *adh* and *aor* expressions are much higher when bacteria grow in mixed
201 condition than in respiration (increased by a factor of 13 for *adh* and 10 for *aor*) indicating a transcriptional
202 regulation. However, the expression of both genes is strongly decreased in the mutant strain, with almost
203 no expression of either gene being detected. Gene expression analysis shows that the deletion of the *hndD*
204 gene drastically impacts the expression of both *adh* and *aor* genes, which is consistent with the findings of
205 the proteomics analysis.

206

207 *Adh level in the periplasmic FeFe-hydrogenase deletion strain*

208 Haveman *et al.* pointed out that, in DvH, in the mutant strain deleted of the periplasmic FeFe-
209 hydrogenase, the *adh* gene is strongly downregulated (Haveman *et al.*, 2003). We compared, using SDS-
210 PAGE, the production of Adh by the *D. fructosovorans* WT strain with the mutant strain that is deleted of its
211 periplasmic FeFe-hydrogenase (SF mutant) (Casalot *et al.*, 2002b) to verify whether, as in DvH, the deletion
212 of this hydrogenase in *D. fructosovorans* has an impact on the level of Adh (Figure S3). In contrast to what
213 was observed in the DvH hydrogenase mutant (Haveman *et al.*, 2003), the amount of Adh in the SF strain is
214 comparable to that present in the WT strain. Furthermore, the SF strain grows as well as the WT strain on
215 PS2 medium (Figure S4). These results suggest that the regulatory mechanisms involved are different in the
216 two *Desulfovibrio* species.

217

218 *Complementation of the hnd deletion*

In order to confirm that the phenotype of the SM4 deletion strain resulted from the absence of the Hnd hydrogenase, complementation analyses were performed. The growth of the complementation strain SM4/pBGhnd6 on PS2 medium is similar to that of WT and SM4 strains (Figure S3). The *hnd* operon is expressed from the pBGhnd6 plasmid in the SM4 strain, as can be observed in Figure 6A showing the relative quantification of *hndD* mRNA levels measured by RT-qPCR. However, in the SM4/pBGhnd6 strain, the expression level does not reach that of the WT strain. Western blot analysis indicates that whereas the level of HndD is very high in the WT strain grown under mixed culture conditions, it is lower in the complementation strain (Figure 5A). Quantification of the intensity of the band corresponding to HndD for the complementation strain on PS2 is almost 2.5 times less intense than for the WT strain. Similarly, the complementation strain produces an intermediate amount of ethanol between that produced by the WT and SM4 strains (Figure 6B). Taken together, these results indicate first that the expression of *hnd* from the pBGhnd6 plasmid does not fully complement the SM4 strain but also that the low expression of *hnd* partially restores ethanol production in this strain.

Discussion

In this study, *D. fructosovorans* WT strain was compared to the SM4 mutant strain lacking Hnd (Δ*hndD*) (Malki *et al.*, 1997) in order to get new insights into the physiological role of this electron-bifurcating hydrogenase when the bacteria grow on pyruvate as a carbon and energy source, under respiratory (PS20 medium) and fermentative (PS0 medium) conditions. We have also tested a mixed culture condition (PS2 medium) using a limiting sulfate concentration, making it possible to reach a higher growth rate as compared to the fermentative condition. After sulfate depletion, the metabolism switches from respiration to fermentation. Under this condition, the *hnd* operon is much more expressed than in the respiratory condition (PS20 medium) (Figure 4). The increase in expression level is followed by an increase in enzyme production as revealed by western blot and in-gel hydrogenase activity detection (Figure 5). This suggests that Hnd hydrogenase plays a role under fermentative conditions.

Deletion of the *hndD* gene leads to a drastic decrease in the expression of the two genes *adh* (DesfrDRAFT_3929) and *aor* (DesfrDRAFT_2487) on PS2 medium, coding respectively for proteins annotated as iron-containing alcohol dehydrogenase (Adh) and aldehyde ferredoxin oxidoreductase (Aor) (Figures 3 and 4). Alcohol dehydrogenases are a group of oxidoreductases that catalyze the interconversion of alcohols to aldehydes or ketones. They are ubiquitous and most of them are NAD- or NADP-dependent enzymes. The size and metal content of Adh vary (for reviews, see (Gaona-Lopez *et al.*, 2016, Radianingtyas & Wright, 2003, Reid & Fewson, 1994)). Adh3929 from *D. fructosovorans* shows high sequence identity with iron-containing alcohol dehydrogenases from various bacteria (52 % with the iron-containing Adh (GI 56552492) from *Zymomonas mobilis* for example) and contains a conserved iron-binding motif ($GX_2HX_2AHX_2GX_5PHG$ where X denotes any amino acid). Adh3929 is highly expressed in *D. fructosovorans* (Figures 3 and 4) and it has been shown previously that it is one of the most abundant enzyme in *Desulfovibrio* (Haveman *et al.*, 2003, Ramos *et al.*, 2015). Ramos *et al*. purified Adh1 (DVU2405) from *D. vulgaris* Hildenborough (DvH), which has 81 % sequence identity to Adh3929, and showed that this enzyme is NAD-dependent and uses ethanol as substrate (Ramos *et al.*, 2015). Aor are tungsten-containing enzymes sensitive to O_2. They catalyze the reversible oxidation of an aldehyde to the corresponding acid using a ferredoxin. Aor2487 from *D. fructosovorans* shows 37% sequence identity with Aor from *Pyrococcus furiosus* whose crystallographic structure has been solved (Chan *et al.*, 1995). These two enzymes Adh and Aor can therefore be involved in the same metabolic pathway since the product of one can be the substrate of the other. Taken together, our data reveal that Hnd is involved in ethanol metabolism when *D. fructosovorans* grows in pyruvate under mixed conditions, which led us to propose a model in which the hydrogenase Hnd would oxidize part of the H_2 produced during fermentation generating both NADH and reduced ferredoxin as a result of its electron bifurcation mechanism (Figure 7). H_2 production results from the release of reducing power in the absence of terminal electron acceptors, enabling the oxidation of pyruvate. In this model, pyruvate would be converted into acetate by the two enzymes pyruvate:ferredoxin oxidoreductase and acetyl-CoA synthase. H_2 could be produced by the membrane hydrogenase Ech from reduced ferredoxin, which would contribute to the electrochemical proton gradient for ATP synthesis. This model proposes that the role of the Hnd hydrogenase would be to produce reducing equivalents (NADH and reduced ferredoxin) from H_2, allowing the production of ethanol by Adh3929 and

271 Aor2487. The lower H_2 production of the WT compared to the SM4 mutant strains is also in agreement with
272 the hypothesis that the physiological role of Hnd when pyruvate is present is thus to consume H_2.

273 The determination of the hydrogenase activity, both H_2-production and H_2-oxidation, on total soluble extracts
274 of WT and SM4 mutant strains grown under mixed condition (PS2) shows that both activities are strongly
275 decreased in the mutant strain (Table S2). It is our assumption that the increased H_2 release in strain SM4
276 (Figure 2) is due to a lack of consumption by Hnd, not an overproduction by Ech. Preliminary proteomic results
277 demonstrate that Ech expression does not vary based on strain or growth condition (data not shown), and
278 there is no indication that its activity would differ between the two strains. In strain SM4, when Hnd is not
279 present, the H_2-production activity measured in the soluble fraction is 44 times less than when is it present in
280 the WT strain (Table S2). Moreover, H_2-oxidation activity shows that strain SM4 consumes 18 times less H_2 than
281 the WT (Table S2) most likely due to the lack of Hnd in this strain.

282 The recently characterized electron-bifurcating hydrogenases were isolated from the anaerobic bacteria
283 *Thermotoga maritima* (Schut & Adams, 2009), *Acetobacterium woodii* (Schuchmann & Müller, 2012), *Moorella*
284 *thermoacetica* (Wang et al., 2013), and *Ruminococcus albus* (Zheng et al., 2014). In the acetogenic bacteria *A.*
285 *woodii* and *M. thermoacetica* which can produce acetate from CO_2 with H_2 as the reductant, these enzymes
286 were found to catalyze the reduction of ferredoxin and NAD^+ with H_2. NADH and reduced ferredoxin are used
287 for CO_2 reduction and to contribute to the ion gradient across the membrane (Schuchmann & Müller, 2012,
288 Wang *et al.*, 2013). In *R. albus* and *T. maritima*, which are glucose fermenting bacteria, trimeric HydABC
289 hydrogenase mediates H_2-production by coupling the endergonic reduction of protons with NADH to the
290 exergonic reduction of protons with reduced ferredoxin (Schut & Adams, 2009, Zheng *et al.*, 2014). *R. albus*, a
291 rumen bacterium, fermentatively produces acetate, ethanol, CO_2 and H_2 in pure culture and in this high H_2-
292 condition, H_2 is mainly generated *via* a ferredoxin-dependent hydrogenase (HydA2). However, *R. albus*
293 redirects carbon flux from ethanol production to the more energetically efficient pathway of acetate
294 production when it grows in co-culture with a hydrogenotrophic bacterium that keeps the H_2 partial pressure
295 sufficiently low through interspecies hydrogen transfer. Under this low H_2-condition, only acetate, CO_2 and H_2
296 are produced. The acetate-only pathway generates more ATP per mole of glucose and equimolar amounts of

297 NADH and reduced ferredoxin, which are then re-oxidized *via* the electron-confurcating HydABC hydrogenase
298 to produce H_2 (Zheng *et al.*, 2014, Greening *et al.*, 2019). *D. fructosovorans,* like *R. albus,* also produces acetate,
299 H_2, ethanol and CO_2 (not measured in this study) when growing on pyruvate in the absence of an electron
300 acceptor. In DvH, ethanol is also a minor product of pyruvate fermentation (Ramos *et al.*, 2015, Traore *et al.*,
301 1981) and the electron flow is redirected towards ethanol when H_2 accumulates at the expense of the
302 energetically more favourable production of acetate (Ramos *et al.*, 2015). However, in *R. albus*, HydABC is
303 responsible for the production of H_2 when the pH_2 is kept very low whereas in *D. fructosovorans*, under
304 fermentative conditions, Hnd is involved in the consumption of H_2 when H_2 accumulates allowing the reduction
305 of NAD^+ for ethanol production.

306 In the WT strain, the expression profile of the three genes *hndD*, *adh* and *aor* is conserved in both PS2 and
307 PS20 media (although *adh* has an expression level that is about twice that of the two genes in PS2) (Figure
308 4) and shows that their expression is much higher in the mixed condition than in the respiration condition.
309 Adh and Aor are thus overproduced when Hnd is overproduced. Their expression is thus strongly regulated
310 at the transcriptional level, but the mechanism of regulation involved remains to be elucidated. Likewise,
311 the molecular basis of the strong drop in *adh* and *aor* expression in the mutant has not yet been
312 deciphered. The drop of Adh level in the SM4 mutant is specific for the deletion of *hnd* in *D. fructosovorans*
313 and is not observed when another FeFe-hydrogenase gene is deleted (in the SF mutant, Figure S3) whereas
314 in DvH, in the periplasmic FeFe-hydrogenase deleted strain, *adh* expression decreases drastically. It should
315 be noted that DvH does not contain any electron-bifurcating hydrogenases.

316 We propose that the regulation of *hnd* expression might be under the control of Rex, which has been
317 described as a global redox-sensing transcriptional repressor that is controlled by the intracellular NAD^+/NADH
318 ratio, a critical indicator for the redox state of the cell. NADH disrupts the interaction of Rex with its respective
319 binding sites, proposed to be induced by a conformational change in the N-terminal domains of the Rex
320 homodimer depending on NAD^+ or NADH binding (Park *et al.*, 2018, Christensen *et al.*, 2015, Brekasis & Paget,
321 2003).Rex has been shown in several bacteria to regulate genes for central metabolism, for proteins involved in
322 energy conversion and in a variety of metabolic processes (Ravcheev *et al.*, 2012). The presence of a predicted

Rex-binding site in the upstream untranslated region of the *hnd* operon (Figure S5) suggests that its expression might be controlled by the intracellular NAD^+/NADH redox state. In DvH, Rex was demonstrated to be a transcriptional repressor of *sat*, a gene encoding for a sulfate adenyl transferase which is involved in sulfate respiration. Surprisingly, *sat* transcript levels were highest when the cells were grown with pyruvate in the absence of sulfate, with the highest levels being found in the Δ*rex* strain, suggesting that Rex induces the expression of genes encoding for proteins that are involved in scavenging sulfate and those that are implicated when the preferred electron acceptor is limiting (Christensen *et al.*, 2015). In *D. fructosovorans*, a putative *rex* gene (DesfrDRAFT_2623) encodes a 24.8 kDa protein that shows 47 % sequence identity with the Rex repressor from *Thermotoga maritima* whose crystallographic structure has been solved (Park *et al.*, 2018). In the anaerobic hyperthermophile bacterium C*aldicellulosiruptor bescii*, structural genes for the NiFe Ech-type hydrogenase and the FeFe Hnd-type hydrogenase are members of the Rex regulon (Sander *et al.*, 2019, Ravcheev *et al.*, 2012). This suggests that Rex may play an important role in H_2 metabolism in this bacterium. In *D. fructosovorans*, the involvement of the putative Rex regulator remains to be determined experimentally. In contrast, a Rex binding site was not found in the promoter of *aor*2487 and *adh3*929, suggesting that although the expression profile of these three genes is similar, their expression is not under the control of the same regulators.

As already mentioned, *D. fructosovorans* harbors a gene cluster for a putative H_2-sensing [FeFe]-hydrogenase, called Hfs or HydS (DesfrDRAFT_3590) whose mechanism has yet to be elucidated. This type of hydrogenase appears to have a regulatory role and the hydrogenase domain containing a non-canonical active site (Chongdar *et al.*, 2018) is fused to a C-terminal PAS domain. The sensory function of HydS has been predicted based on the presence of this PAS domain (Greening *et al.*, 2016). PAS domains are widely utilized for various signal transduction and sensory functions (Henry & Crosson, 2011) and are frequently found in signal transduction cascades involving serine/threonine protein kinases and phosphatases. Transcriptional studies of *R. albus* have provided some insights into the regulatory function of HydS (Zheng *et al.*, 2014). In this bacterium, the genes encoding for HydS are co-transcribed with the transcriptional repressor Rex and the ferredoxin-dependent [FeFe]-hydrogenase HydA2, whereas ~~there is an~~ genes encoding the electron-bifurcating hydrogenase HydABC are located on a separate operon (Zheng *et al.*,

2014). It is likely that HydS, in tandem with Rex, is sensing the NADH/NAD^+ ratio of the cell *via* the H_2 partial pressure, with the ratio being higher at high H_2 concentrations, and modulating the transcription of genes so that the NADH/NAD^+ ratio is balanced (Zheng *et al.*, 2014). Greening *et al*. also proposed that in *R. albus*, FeFe-hydrogenases are regulated by HydS as a result of direct H_2-sensing (Greening *et al.*, 2019). It is of note that the presence of a *hydS* gene in the genome of *Desulfovibrio* species is always correlated with the presence of *hnd* genes (Baffert *et al.*, 2019). The coexistence of multimeric [FeFe]-hydrogenases and HydS is also found in other H_2-forming bacteria such as in *Thermoanaerobacterium saccharolyticum*, *Thermoanaerobacter tengcongensis* and *Thermotoga maritima* (Chongdar *et al.*, 2018, Pan *et al.*, 2003, Shaw *et al.*, 2009, Soboh *et al.*, 2004) however the extent of the role of HydS in the regulatory cascade still needs to be clarified.

In DvH, an hexameric NADH dehydrogenase/heterodisulfide reductase complex Hdr-Flx is involved in ethanol metabolism. Strains mutated in genes that encode the proteins of this complex also produce a reduced amount of ethanol compared to the WT strain during pyruvate fermentation (Ramos *et al.*, 2015). The Hdr-Flx complex is proposed to be essential for NADH oxidation during growth on ethanol, probably using an electron bifurcation mechanism that leads to the reduction of a ferredoxin and a small protein, DsrC, involved in sulfate reduction, whereas during fermentation, the complex would function in the opposite direction reducing NAD^+ for ethanol production (Ramos *et al.*, 2015). In *D. fructosovorans*, the 7 genes encoding this complex are present in the genome immediately downstream of the *adh* gene (desfrDRAFT_3930 to 3936), suggesting that it may also be involved in ethanol metabolism but its role in *D. fructosovorans* remains to be determined.

In conclusion, we demonstrated that the electron-bifurcating hydrogenase Hnd is involved in ethanol metabolism in *D. fructosovorans* in pyruvate medium under fermentative conditions. The deletion of the *hnd* gene has a drastic effect on the expression of both *adh* and *aor* genes. Although the link between the deletion of *hnd* and the decrease in the expression of both *adh* and *aor* as well as the regulatory mechanisms at play remain to be understood, this study nevertheless provides a significant advance in the function of Hnd in *D. fructosovorans*.

Experimental procedures

Bacterial strains and growth conditions.

The WT strain of *Desulfovibrio fructosovorans* DSM 3604 (Ollivier *et al.*, 1988) and the two mutants, SM4 and SF strains, which are deleted of *hndD* encoding the hydrogenase catalytic subunit of Hnd (Δ*hndD*, Cm^R) (Malki *et al.*, 1997) or of *hydAB* encoding the small and large subunits of the periplasmic [FeFe]-hydrogenase (Δ*hydAB*, Gm^R) (Casalot *et al.*, 2002b), respectively, were used in this study. To complement the deletion strain SM4, the pBGhnd6 plasmid containing the entire *hnd* operon including the promoter region (600 bp) was constructed and used to transform the SM4 strain as previously described (Kpebe *et al.*, 2018) to produce the SM4/pBGhnd6 strain.

Strains were grown anaerobically at 37°C in different media. The basal medium (pH 6.8) contains 25 mM sodium pyruvate, 8 mM NH_4Cl, 1.3 mM $CaCl_2$, 17.1 mM NaCl, 6.7 mM KCl, 2.1 mM $MgCl_2$ and trace elements (Rousset *et al.*, 1998) and corresponds to the PS0 medium. Na_2SO_4 was added to the basal medium to obtain the PS20 medium containing 20 mM sulfate. $MgCl_2$ and $CaCl_2$ in the basal medium were replaced by 1 mM $CaSO_4$ and 1 mM $MgSO_4$ to obtain the PS2 medium containing 2 mM sulfate. Prior to inoculation, 20 mM KH_2PO_4 pH 6.8, 2.5 mM Na_2S and 10 mM $NaHCO_3$ were added. Thiamphenicol (35 µg/mL) or gentamicin (20 µg/mL) were added to the SM4 or SF mutant culture media. The media were inoculated with 5% (v/v) of fresh cultures.

Hydrogen production measurement

Cells were grown in 100 mL bottles containing 90 mL of PS0, PS2 or PS20 medium. The media were inoculated with fresh cultures of WT or SM4 strains grown on PS2 medium. Each culture was done in triplicate. For H_2 quantification, 100 µL of headspace gas was removed periodically using a gastight syringe and injected into a gas chromatography system (Agilent 7820A) equipped with a thermal conductivity detector and a GS-Carbonplot 115-3133 column (30 m, 530 µm, 3 µm), using nitrogen as the carrier gas, at

400 a flow rate of 8.2 ml/min, an oven temperature of 30 °C and a detector temperature of 200 °C. The H_2
401 production is expressed as micromols of H_2 accumulated in the headspace.

402 *HPLC analysis*

403 Acetate production, pyruvate and ethanol consumption were followed by HPLC. The analysis was
404 performed on the same *D. fructosovorans* cultures as those used to measure H_2 production and as those
405 used for the growth curves. 1 mL of culture samples were collected at different growth phase, centrifuged
406 at 14 100 g for 6 min to remove the cells, filtered through a 0.22 µm filter and stored at -20°C until use.
407 Immediately before the analysis, 10 µL of H_2SO_4 0,5 M were added to 490 µL of sample to obtain a final
408 concentration of 10 mM of H_2SO_4 and the samples were centrifugated for 5 min. The analysis was carried
409 out on an Agilent 1200 HPLC system equipped with a refractometer (Agilent Technologies). Acetate,
410 ethanol and pyruvate separation was achieved with an Agilent Hi-Plex H column (300 x 7.7mm) set at 50 °C.
411 25 µL of samples were injected. The compounds were eluted with 10mM sulfuric acid mobile phase at a
412 flow rate of 0.6 $mL.min^{-1}$.

413 *Ethanol quantification with an enzymatic kit*

414 When indicated, ethanol production in the growth medium was determined with an enzymatic kit
415 from Boehringer Mannheim/R-Biopharm according to the manufacturer instructions. This method is based
416 on quantifying NADH formed from ethanol through the combined action of Adh and aldehyde
417 dehydrogenase.

418 *Sulfate determination*

419 The concentration of sulfate was measured using a turbidimetric method previously described
420 (Marietou *et al.*, 2009), based on the reaction of sulfate with barium chloride, resulting in the precipitation
421 of barium sulfate. At different growth times, 5 mL culture samples were harvested, 0.22 µm filter-sterilized
422 and stored at 4°C. 100 µL of these samples were added to 900 µL of conditioning agent (10.2 mM glycerol,
423 6 mM concentrated HCl, 22.3 mM NaCl, 1.7 % ethanol) and 100 µL of 1 M barium chloride. The solution was
424 then vortexed for 30 s and incubated at room temperature for 45 min to allow the precipitation of barium

sulfate. The absorbance of the solution at 420 nm was determined and the concentration of sulfate in the samples was calculated from the calibration curve prepared using standard solutions of sodium sulfate.

Separation of proteins by SDS-PAGE

D. fructosovorans cells were grown in 1L bottles containing 900 mL medium, harvested at the end of exponential phase of growth by centrifugation. The cell pellet was resuspended in buffer Tris-HCl 20 mM pH 7.6 supplemented with protease inhibitors (SIGMAFAST™ Protease Inhibitor Cocktail Tablet, Sigma-Aldrich), DNase I (Roche) and Lysozyme (Sigma-Aldrich). Cells were disrupted by two passages through a chilled French press cell at a pressure of 100 MPa. After an ultracentrifugation at 200 000 g for 45 min at 4°C, proteins were separated on 10% polyacrylamide denaturing gels (SDS-PAGE) using a mini VE electrophoresis apparatus (Amersham Pharmacia). After migration, gel was stained with Coomassie blue staining solution (20% ethanol, 10% acetic acid and 0.15% Coomassie blue R250) and destained by soaking for at least two hours in a solution of ethanol/acetic acid/water (20:10:70 vol/vol/vol).

Blue-Native gel (BN-gel) electrophoresis and in-gel hydrogenase activity detection

D. fructosovorans cells were grown in 1L bottles containing 900 mL medium, harvested at the end of exponential phase of growth by centrifugation. Periplasmic extract was removed from the soluble sample to avoid periplasmic hydrogenase activity bands on the BN gel. The cell pellet was resuspended in 5 mL TRIS-HCL 50 mM pH 9, sodium carbonate 170 mM, EDTA 50 mM and incubate 30 min at 30°C under gentle agitation (100 RPM). After centrifugation for 20 min at 20000 g, the incubation step was repeated another time in the same condition. The cell pellet was then used to prepare the soluble extract as described for the SDS-PAGE. BN gels were performed on 5-13% acrylamide gradient gel, according to the method of Schägger (Schägger *et al.*, 1994, Schägger & von Jagow, 1991), as described by Le Laz et al. (2014) (Le Laz *et al.*, 2014). In-gel hydrogenase activity was detected as described previously by Kpebe et al. (2018) (Kpebe *et al.*, 2018) using methyl viologen as electron acceptor.

Western immunoblots

D. fructosovorans cells were grown in 100 mL bottles containing 90 mL of PS2 or PS20 medium. When indicated, sulfate was replaced by 2 or 20 mM sodium thiosulfate, or 4 or 40 mM sodium fumarate. Cells were harvested at late exponential phase or stationary phase of growth. Cells were disrupted at 100°C for 10 min in a loading buffer in the presence of 215 mM β-mercaptoethanol, 15 mM DTT and 2 % SDS and the extracts were centrifuged at 14 000g for 10 min. Soluble proteins in the supernatant were quantified with the Bio-Rad protein assay based on Bradford dye binding method, using bovine serum albumin (BSA) as a standard. Proteins were separated by 10% SDS-PAGE and electrotransferred to a nitrocellulose membrane (Fastblot, Biometra). The membrane was blocked for 1 h in TBST (500 mM Tris-HCl pH 7.5, 1.5 M NaCl, 0.2% Tween 20) containing 5% skim milk and incubated overnight at 4°C with a 5000-fold dilution of the primary rabbit anti-HndD antibody in the same buffer. After three 10 min washes in TBST, the membrane was developed using a 1/20 000 dilution of horseradish peroxidase-conjugated goat anti-rabbit secondary antibody for 1 h and the ECL western blotting detection reagents (Amersham). The primary anti-HndD antibody was generated by Eurogentec from a rabbit immunized with gel purified his-tagged HndD protein. IgG from serum were purified by affinity chromatography (protein G Sepharose, GE Healthcare). Protein loading was controlled by performing two identical SDS-PAGE in parallel. The first one was used for western immunoblotting experiment while the second one was stained with Coomassie blue staining solution. Protein quantification was done with Image J free software (NIH, LOCI, University of Wisconsin) (Schneider *et al.*, 2012).

Protein Identification by In-gel Digestion and Mass Spectrometry

Gel electrophoresis bands of proteins from SDS-PAGE were put into a 96-well microplate (Greiner) and in-gel trypsin digestion of proteins was performed according to Guiral et al. (2009) (Guiral *et al.*, 2009). Proteins were identified by LC-MSMS as described previously by Guiral et al (2009) (Guiral *et al.*, 2009) except that the peptides were separated by one dimension liquid chromatography on the reversed-phase column C18 only, and that the proteins analysed here are soluble proteins instead of membrane proteins. The database *Desulfovibrio fructosovorans* (TxID 878, 4701 entries) used was extracted from NCBI.

Hydrogenase activity in total soluble extracts

475 *Preparation of soluble extracts*

476 *D. fructosovorans* cells, grown in 1 L bottles containing 900 mL of PS2 medium were harvested at
477 the end of the exponential phase and resuspended in 10 mL of 100 mM Tris-HCl pH 8 supplemented with
478 protease inhibitors (SIGMAFAST™ Protease Inhibitor Cocktail Tablet, Sigma-Aldrich), DNase I (Roche) and
479 Lysozyme (Sigma-Aldrich). The cells were broken in an anaerobic glovebox (Jacomex) using a sonicator
480 (Hielscher) in 10 cycles of 1 minute of sonication then 1 minute of rest in a water bath chilled at 4°C. The
481 cell extract was ultracentrifuged at 200 000 g for 45 min at 4°C, then the soluble fraction was recovered,
482 and the total protein was quantified using the Bio-Rad protein assay based on Bradford dye binding
483 method, using bovine serum albumin (BSA) as a standard.

484 *H_2 evolution assays*

485 H_2 evolution assays were carried out using dithionite-reduced methyl viologen (50 mM reduced
486 with 23 mM sodium dithionite) as electron donor, in anaerobic 6.5 mL-serum bottles containing 1 mL
487 reaction mixture composed of Tris-HCl 0.1 M pH8, at 30°C. The gas phase was 100% N_2. The reaction was
488 started by the addition of 26.3 µg proteins of WT *D. fructosovorans* soluble extract or 226.5 to 377.5 µg
489 proteins of SM4 strain soluble extract. H_2 production was measured using gas chromatography (GC). Fifty
490 microliters of headspace gas was removed periodically from the vials using a gastight syringe and injected
491 into a GC system (Agilent 7820) equipped with a thermal conductivity detector and a Carbon-plot capillary
492 column (30 m, 0.53 mm, 3 µm), using nitrogen as the carrier gas, at a flow rate of 8.15 mL/min, an oven
493 temperature of 30 °C and a detector temperature of 200 °C. One unit of hydrogenase activity corresponds
494 to the production of 1 µmol of H_2/min.

495 *H_2 oxidation assays*

496 H_2-oxidizing activity measurements were performed in anaerobic quartz cuvettes, under 1 bar-
497 pressure of $_{H2,}$ in 800 µL of reaction mixture containing 100mM Tris-HCl pH 8.0, 2mM dithiothreitol (DTT),
498 and 50mM methyl viologen (Sigma Aldrich) as artificial electron acceptor. The reaction was started by the
499 addition of 0.5 to 7.5 µg proteins of WT *D. fructosovorans* soluble extract or SM4 strain soluble extract to

the mixture to start the reaction and methyl viologen reduction was monitored at 604 nm (ε=13,600$M^{-1}.cm^{-1}$) using a UV-Vis spectrophotometer Lambda 25 (Perkin Elmer). One unit of hydrogenase activity corresponds to the uptake of 1 µmol of H_2/min.

RNA preparation

D. fructosovorans cells, grown in 2 L bottles containing 1.8 L of PS2 or PS20 medium, were harvested at the end of the exponential phase of growth. 10^{10} cells were pelleted, washed three times, and resuspended in 200 µL of 10 mM Tris-HCl, pH 8. Total RNA was prepared using the High Pure RNA kit from Roche Diagnostics according to the manufacturer's instructions. To remove genomic DNA contamination, total RNA was then treated with the TURBO DNA-free™ kit (Life Technologies). RNA concentration and purity were determined with a NanoDrop 2000 spectrophotometer (Thermo Scientific) and electrophoretic migration on an agarose gel was performed to verify the absence of RNA degradation. The absence of contaminant DNA was verified by PCR with the *Taq* DNA-dependent DNA polymerase (Fermentas) using *16S* specific primers (16S-F and 16S-R, Table S3).

Real-time quantitative PCR (RT-qPCR).

Reverse transcription was performed on 500 ng of total RNA by using the SuperScriptIII reverse transcriptase and random primers (Invitrogen). Real-time PCR runs were carried out on a CFX96 Real time System (Bio-Rad). Cycling parameters of the real time PCR were 98°C for 2 min, followed by 45 cycles of 98°C for 5 s and 60°C for 10 s, ending with a melting curve analysis from 65°C to 95°C to determine the specificity of the amplification. To determine the amplification kinetics of each product, the fluorescence derived from the incorporation of EvaGreen into the double-stranded PCR products was measured at the end of each cycle using the SsoFast™ EvaGreen® Supermix 2X Kit (Bio-Rad). The results were analyzed using the Bio-Rad CFX Manager Software 3.0. The 16S rRNA gene was used as a reference for normalization. The real-time quantitative PCR experiments were performed in duplicate assays with total RNA from at least three independent growth experiments. Primers used for the real time PCR are listed in Table S3.

Acknowledgements

Our work is supported by CNRS and Aix Marseille Université. This project has received funding from the European Union's Horizon 2020 research and innovation programme under the Marie Skłodowska-Curie grant agreement No713750. Also it has been carried out with the financial support of the Regional Council of Provence-Alpes-Côtes d'Azur and with the financial support of the A*MIDEX (n° ANR- 11-IDEX-0001-02), funded by the Investissements d'Avenir project funded by the French Government, managed by the French National Research Agency (ANR). The authors thank Marianne Guiral, Ariane Atteia and Sébastien Le Laz for fruitful discussions and Cassandra Backes for help with HPLC experiments.

The authors have no conflict of interest to declare.

Author Contributions

Conception and design of the study: MB and LS; acquisition, analysis, or interpretation of the data, NP, AK, CG, CB, JR, RL and YD, LS and MB; writing of the manuscript: MB, NP and AK. All authors reviewed the manuscript.

Figure legends

Figure 1: Growth curves of *Desulfovibrio fructosovorans* WT and SM4 strains. Bacteria were grown in PS0 (A, fermentation), PS2 (B, mixed culture condition) and PS20 (C, respiration) media containing no, 2 mM and 20 mM sulfate respectively and 25 mM pyruvate as electron donor. WT strain, black curves; SM4 strain, red curves. OD600 was followed as a function of time. OD units were converted into number of cells (1 mL of cells at OD600 of 1 represents 10^9 cells). Data represent the averages of the results of three replicate growths. Error bars correspond to standard deviations.

Figure 2: Pyruvate, acetate, ethanol and H_2 quantification. Pyruvate (open squares), acetate (closed triangles) and ethanol (closed circles) in the growth medium and H_2 (open diamonds) in the headspace were quantified by HPLC or GC during the growth of the *D. fructosovorans* WT strain (black curves) or SM4

549 mutant strain (red curves) under fermentation (PS0, A and D), mixed culture condition (PS2, B and E) or
550 respiration (PS20, C and F). Analysis were performed on the same *D. fructosovorans* cultures as those used
551 for the growth curves. Times indicated on the x-axis correspond to those in Figure 1. Data represent the
552 averages of the results of three replicate growths. Error bars correspond to standard deviations.

553 Figure 3: Proteomic analysis. (A) Separation by Coomassie-blue-stained SDS-PAGE of soluble proteins from
554 WT (lanes 1 and 3) and SM4 mutant (lanes 2 and 4) strains of *Desulfovibrio fructosovoran*s grown under
555 mixed (lanes 1 and 2) or respiratory (lanes 3 and 4) conditions. Cells were harvested at the end of the
556 exponential phase. 45 µg of soluble proteins were loaded in each lane of a 10 % SDS-PAGE. Molecular mass
557 markers (lane 5) are indicated in kDa. (B) Proteins identified by mass spectrometry (ion trap MS/MS) in
558 bands showing a different intensity in the two strains. Data correspond to identified proteins in bands 1, 2
559 and 3 from WT cells grown under mixed condition (panel A, lane 1). Only proteins identified with the
560 highest score in each gel band are reported (for the complete list of identified proteins, see Table S1). Table
561 heading: Protein name, protein name in NCBI database. NCBI entry, accession number. Unique peptides:
562 number of distinct peptides matching to protein sequence and unique to this protein. Sequence coverage,
563 protein sequence coverage by the matching peptides (in %). Theor. M_r, theoretical molecular mass in kDa of
564 the identified protein. These results are representative of several similar experiments.

565 Figure 4: Relative expression of the *adh*, *aor* and *hndD* genes quantified by RT-qPCR. *D. fructosovorans* WT
566 and SM4 strains were grown under mixed culture condition (PS2 medium) or under respiratory condition
567 (PS20 medium) and samples were collected at the end of the exponential phase of growth. Expression of
568 the genes was normalized to that of the 16S rRNA gene. These results are representative of several similar
569 experiments.

570 Figure 5: Hnd hydrogenase production and detection of its activity on BN-gel. (A) Western blot analysis of
571 HndD production by WT (lanes 1 and 2), SM4 (lane 3) and SM4/pBGhnd6 (lane 4) cells of *D. fructosovorans*
572 grown in medium containing 2 mM (PS2) (lanes 1, 3 and 4) or 20 mM (PS20) (lane 2) sulfate. Cells were
573 harvested at stationary phase of growth and 25 µg of total proteins from whole-cell protein extracts were
574 separated by 10% SDS-PAGE and subjected to Western blotting using an antibody raised against HndD. The

SDS-PAGE gel below the western blot is a loading control. (B) In-gel detection of hydrogenase activity in on BN-gel of cytoplasmic proteins prepared from *D. fructosovorans* WT strain grown on PS20 (lane 1) or PS2 (lane 2) medium. 35 µg of cytoplasmic proteins were loaded on a 5–13% polyacrylamide gel. Molecular weight markers are indicated in kDa (lane 3).

Figure 6: Relative *hndD* gene expression and production of ethanol by *D. fructosovorans* WT strain and the complementation strain SM4/pBGhnd6 grown under mixed culture condition (PS2 medium). Samples were collected at the end of the exponential phase of growth. (A) Relative expression of the *hndD* gene quantified by RT-qPCR. Expression of the gene was normalized to that of the 16S rRNA gene. Error bars correspond to standard deviations. (B) Ethanol concentration in the growth medium quantified with an enzymatic kit. These results are representative of several similar experiments.

Figure 7: Model of the pyruvate oxidation pathway by *D. fructosovorans* under pyruvate fermentation conditions. Pyruvate is converted into acetate by the 2 enzymes Pfo and Acs. Part of the acetate is converted into ethanol by Aor and Adh. H_2 could be produced by the membrane NiFe-hydrogenase Ech from reduced ferredoxin, which would contribute to the electrochemical proton gradient for ATP synthesis. This model proposes that the role of the Hnd hydrogenase would be to produce reducing equivalents (NADH and reduced ferredoxin) from H_2, allowing the production of ethanol. Pfo, pyruvate ferredoxin oxidoreductase; Acs, Acetyl-CoA synthase; Aor, Aldehyde ferredoxin oxidoreductase; Adh, Alcohol dehydrogenase; Ech and Hnd, Hydrogenases. Fd_{ox}, oxidized ferredoxin; Fd^{2-}, reduced ferredoxin. This figure was created with BioRender.com.

Figure S1: Growth curve, sulfate consumption and H_2 production by *D. fructosovorans* WT cells. Bacteria were grown in PS2 medium (mixed culture condition). Sulfate concentration in the growth medium was determined using a turbidimetric method with barium chloride. H_2 in the headspace was quantified using GC. H_2 starts to accumulate when sulfate is completely reduced.

Figure S2: Western blot analysis of HndD production by *D. fructosovorans* WT cells grown in medium containing 25 mM pyruvate and 20 mM thiosulfate (lane 1), 2 mM thiosulfate (lane 2), 40 mM fumarate

600 (lane 3) or 4 mM fumarate (lane 4) as electron acceptor. Cells were harvested at late exponential phase of
601 growth and 2 µg of total proteins from whole-cell protein extracts were separated by 10% SDS-PAGE and
602 subjected to western blotting using an antibody raised against HndD. The SDS-PAGE gel below the western
603 blot is a loading control.

604 Figure S3: Separation by Coomassie-blue-stained SDS-PAGE of soluble proteins from WT (lane 2), SM4
605 mutant (lane 3) and SF mutant (lane 4) strains of *Desulfovibrio fructosovoran*s grown under mixed
606 conditions (PS2). Cells were harvested at the end of the exponential phase. 45 µg of soluble proteins were
607 loaded in each lane of a 10 % SDS-PAGE. Molecular mass markers (lane 1) are indicated in kDa.

608 Figure S4: Growth curves of *Desulfovibrio fructosovorans* WT, SM4 (Δ*hndD*), SM4/pBGhnd6 and SF
609 (Δ*hydAB*) strains. Bacteria were grown in PS2 medium containing 25 mM pyruvate as electron donor and 2
610 mM sulfate as electron acceptor (mixed culture condition).

611 Figure S5: Predicted Rex binding-site in the promoter region of *hnd*. (A) Sequence logo of the DNA
612 recognition motif for all Rex sites in the order Desulfovibrionales. The sequence logo was constructed
613 based on the alignment of 117 sites identified as Rex recognition sequences (available in the RegPrecise
614 database). (B) Consensus sequence of the Rex binding sites in the promoter region of the tetrameric,
615 cytoplasmic [FeFe] hydrogenases found in *Desulfovibrio.* The consensus sequence was constructed by
616 aligning the known sites with ClustalW multiple alignment. (C) The Rex binding sites and their locations in
617 the promoter region of the tetrameric, cytoplasmic [FeFe] hydrogenases in *Desulfovibrio* species. The
618 promoter region sequences were taken from NCBI and the Rex-binding site was mapped. Identical residues
619 between the species are highlighted in red.

620

Table

Table 1: Growth parameters of WT and SM4 *D. fructosovorans* strains.

Medium		Doubling time (h)		Maximum cell count/mL†	
		WT	SM4	WT	SM4
PS0		369.0±73.5	519.5±100.7	$6.90\times10^{8} \pm 4.0\times10^{7}$	$6.70\times10^{8} \pm 3.0\times10^{7}$
PS2	**Phase 1** 0-40 hrs	17.2±0.9	17.4±5.7	$1.12\times10^{9} \pm 1.0\times10^{7}$	$1.16\times10^{9} \pm 2.0\times10^{7}$
	Phase 2 40-110 hrs	89.3±3.5	114.2±1.1		
PS20		20.5±0.3	15.3±1.2	$1.33\times10^{9} \pm 1.0\times10^{7}$	$1.41\times10^{9} \pm 4.0\times10^{7}$

† The highest optical density at 600 nm was converted into number of cells (1 mL of cells at OD600 of 1 represents 10^9 cells). Data are mean values +/- standard deviation and were obtained from triplicate separated experiments.

References

Baffert, C., Kpebe, A., Avilan, L., and Brugna, M. (2019) Hydrogenases and H_2 metabolism in sulfate-reducing bacteria of the *Desulfovibrio genus*. *Advances in microbial physiology* **74**: 143-189.

Benoit, S.L., Maier, R.J., Sawers, R.G., and Greening, C. (2020) Molecular Hydrogen Metabolism: a Widespread Trait of Pathogenic Bacteria and Protists. *Microbiology and molecular biology reviews : MMBR* **84**.

Brekasis, D., and Paget, M.S. (2003) A novel sensor of NADH/NAD+ redox poise in *Streptomyces coelicolor* A3(2). *The EMBO journal* **22**: 4856-4865.

Bryant, M.P., Campbell, L.L., Reddy, C.A., and Crabill, M.R. (1977) Growth of *Desulfovibrio* in lactate or ethanol media low in sulfate in association with H_2-utilizing methanogenic bacteria. *Appl Environ Microbiol* **33**: 1162-1169.

Buckel, W., and Thauer, R.K. (2018a) Flavin-Based Electron Bifurcation, A New Mechanism of Biological Energy Coupling. *Chem Rev*.

Buckel, W., and Thauer, R.K. (2018b) Flavin-Based Electron Bifurcation, Ferredoxin, Flavodoxin, and Anaerobic Respiration With Protons (Ech) or NAD(+) (Rnf) as Electron Acceptors: A Historical Review. *Frontiers in microbiology* **9**: 401.

Casalot, L., De Luca, G., Dermoun, Z., Rousset, M., and de Philip, P. (2002a) Evidence for a fourth hydrogenase in *Desulfovibrio fructosovorans*. *Journal of bacteriology* **184**: 853-856.

Casalot, L., Hatchikian, C.E., Forget, N., de Philip, P., Dermoun, Z., Belaich, J.P., and Rousset, M. (1998) Molecular study and partial characterization of iron-only hydrogenase in *Desulfovibrio fructosovorans*. *Anaerobe* **4**: 45-55.

Casalot, L., Valette, O., De Luca, G., Dermoun, Z., Rousset, M., and de Philip, P. (2002b) Construction and physiological studies of hydrogenase depleted mutants of *Desulfovibrio fructosovorans*. *FEMS microbiology letters* **214**: 107-112.

Chan, M.K., Mukund, S., Kletzin, A., Adams, M.W., and Rees, D.C. (1995) Structure of a hyperthermophilic tungstopterin enzyme, aldehyde ferredoxin oxidoreductase. *Science* **267**: 1463-1469.

Chongdar, N., Birrell, J.A., Pawlak, K., Sommer, C., Reijerse, E.J., Rudiger, O., Lubitz, W., and Ogata, H. (2018) Unique Spectroscopic Properties of the H-Cluster in a Putative Sensory [FeFe] Hydrogenase. *Journal of the American Chemical Society* **140**: 1057-1068.

Christensen, G.A., Zane, G.M., Kazakov, A.E., Li, X., Rodionov, D.A., Novichkov, P.S., Dubchak, I., Arkin, A.P., and Wall, J.D. (2015) Rex (encoded by DVU_0916) in *Desulfovibrio vulgaris* Hildenborough is a repressor of sulfate adenylyl transferase and is regulated by NADH. *Journal of bacteriology* **197**: 29-39.

de Luca, G., de Philip, P., Rousset, M., Belaich, J.P., and Dermoun, Z. (1998) The NADP-reducing hydrogenase of *Desulfovibrio fructosovorans*: evidence for a native complex with hydrogen-dependent methyl-viologen-reducing activity. *Biochemical and biophysical research communications* **248**: 591-596.

Fauque, G., Peck, H.D., Jr., Moura, J.J., Huynh, B.H., Berlier, Y., DerVartanian, D.V., Teixeira, M., Przybyla, A.E., Lespinat, P.A., Moura, I., and et al. (1988) The three classes of hydrogenases from sulfate-reducing bacteria of the genus *Desulfovibrio*. *FEMS microbiology reviews* **4**: 299-344.

Gaona-Lopez, C., Julian-Sanchez, A., and Riveros-Rosas, H. (2016) Diversity and Evolutionary Analysis of Iron-Containing (Type-III) Alcohol Dehydrogenases in Eukaryotes. *PloS one* **11**: e0166851.

Greening, C., Biswas, A., Carere, C.R., Jackson, C.J., Taylor, M.C., Stott, M.B., Cook, G.M., and Morales, S.E. (2016) Genomic and metagenomic surveys of hydrogenase distribution indicate H_2 is a widely utilised energy source for microbial growth and survival. *The ISME journal* **10**: 761-777.

Greening, C., Geier, R., Wang, C., Woods, L.C., Morales, S.E., McDonald, M.J., Rushton-Green, R., Morgan, X.C., Koike, S., Leahy, S.C., Kelly, W.J., Cann, I., Attwood, G.T., Cook, G.M., and Mackie, R.I. (2019) Diverse hydrogen production and consumption pathways influence methane production in ruminants. *The ISME journal* **13**: 2617-2632.

Guiral, M., Prunetti, L., Lignon, S., Lebrun, R., Moinier, D., and Giudici-Orticonit, M.T. (2009) New insights into the respiratory chains of the chemolithoautotrophic and hyperthermophilic bacterium *Aquifex aeolicus*. *Journal of proteome research* **8**: 1717-1730.

Hatchikian, C.E., Traore, A.S., Fernandez, V.M., and Cammack, R. (1990) Characterization of the nickel-iron periplasmic hydrogenase from *Desulfovibrio fructosovorans*. *Eur J Biochem* **187**: 635-643.

Haveman, S.A., Brunelle, V., Voordouw, J.K., Voordouw, G., Heidelberg, J.F., and Rabus, R. (2003) Gene expression analysis of energy metabolism mutants of *Desulfovibrio vulgaris* Hildenborough indicates an important role for alcohol dehydrogenase. *Journal of bacteriology* **185**: 4345-4353.

Henry, J.T., and Crosson, S. (2011) Ligand-binding PAS domains in a genomic, cellular, and structural context. *Annual review of microbiology* **65**: 261-286.

Higuchi, Y., Yagi, T., and Yasuoka, N. (1997) Unusual ligand structure in Ni-Fe active center and an additional Mg site in hydrogenase revealed by high resolution X-ray structure analysis. *Structure* **5**: 1671-1680.

Keller, K.L., and Wall, J.D. (2011) Genetics and molecular biology of the electron flow for sulfate respiration in *Desulfovibrio*. *Frontiers in microbiology* **2**: 135.

Kpebe, A., Benvenuti, M., Guendon, C., Rebai, A., Fernandez, V., Le Laz, S., Etienne, E., Guigliarelli, B., Garcia-Molina, G., de Lacey, A.L., Baffert, C., and Brugna, M. (2018) A new mechanistic model for an O_2-protected electron-bifurcating hydrogenase, Hnd from *Desulfovibrio fructosovorans*. *Biochimica et biophysica acta. Bioenergetics* **1859**: 1302-1312.

Le Laz, S., Kpebe, A., Bauzan, M., Lignon, S., Rousset, M., and Brugna, M. (2014) A biochemical approach to study the role of the terminal oxidases in aerobic respiration in *Shewanella oneidensis* MR-1. *PloS one* **9**: e86343.

Malki, S., De Luca, G., Fardeau, M.L., Rousset, M., Belaich, J.P., and Dermoun, Z. (1997) Physiological characteristics and growth behavior of single and double hydrogenase mutants of *Desulfovibrio fructosovorans*. *Arch Microbiol* **167**: 38-45.

Malki, S., Saimmaime, I., De Luca, G., Rousset, M., Dermoun, Z., and Belaich, J.P. (1995) Characterization of an operon encoding an NADP-reducing hydrogenase in Desulfovibrio fructosovorans. *Journal of bacteriology* **177**: 2628-2636.

703 Marietou, A., Griffiths, L., and Cole, J. (2009) Preferential reduction of the thermodynamically less favorable
704 electron acceptor, sulfate, by a nitrate-reducing strain of the sulfate-reducing bacterium
705 *Desulfovibrio desulfuricans* 27774. *Journal of bacteriology* **191**: 882-889.
706 Meyer, B., Kuehl, J., Deutschbauer, A.M., Price, M.N., Arkin, A.P., and Stahl, D.A. (2013a) Variation among
707 *Desulfovibrio* species in electron transfer systems used for syntrophic growth. *Journal of*
708 *bacteriology* **195**: 990-1004.
709 Meyer, B., Kuehl, J.V., Deutschbauer, A.M., Arkin, A.P., and Stahl, D.A. (2013b) Flexibility of syntrophic
710 enzyme systems in *Desulfovibrio* species ensures their adaptation capability to environmental
711 changes. *Journal of bacteriology* **195**: 4900-4914.
712 Nicolet, Y., Piras, C., Legrand, P., Hatchikian, C.E., and Fontecilla-Camps, J.C. (1999) *Desulfovibrio*
713 *desulfuricans* iron hydrogenase: the structure shows unusual coordination to an active site Fe
714 binuclear center. *Structure* **7**: 13-23.
715 Noguera, D.R., Brusseau, G.A., Rittmann, B.E., and Stahl, D.A. (1998) A unified model describing the role of
716 hydrogen in the growth of *Desulfovibrio vulgaris* under different environmental conditions.
717 *Biotechnology and bioengineering* **59**: 732-746.
718 Odom, J.M., and Peck, H.D., Jr. (1981) Hydrogen cycling as a general mechanism for energy coupling in the
719 sulfate-reducing bacteria, *Desulfovibrio* sp. *FEMS Microbiol Letters* **12**: 47-50.
720 Ollivier, B., Cord-Ruwisch, R., Hatchikian, E.C., and Garcia, J.L. (1988) Characterization of *Desulfovibrio*
721 *fructosovorans* sp. nov. *Arch Microbiol* **149**: 447-450.
722 Pan, G., Menon, A.L., and Adams, M.W. (2003) Characterization of a [2Fe-2S] protein encoded in the iron-
723 hydrogenase operon of Thermotoga maritima. *Journal of biological inorganic chemistry : JBIC : a*
724 *publication of the Society of Biological Inorganic Chemistry* **8**: 469-474.
725 Park, Y.W., Jang, Y.Y., Joo, H.K., and Lee, J.Y. (2018) Structural Analysis of Redox-sensing Transcriptional
726 Repressor Rex from *Thermotoga maritima*. *Scientific reports* **8**: 13244.
727 Pereira, I.A., Ramos, A.R., Grein, F., Marques, M.C., da Silva, S.M., and Venceslau, S.S. (2011) A comparative
728 genomic analysis of energy metabolism in sulfate reducing bacteria and archaea. *Frontiers in*
729 *microbiology* **2**: 69.
730 Peters, J.W., Lanzilotta, W.N., Lemon, B.J., and Seefeldt, L.C. (1998) X-ray crystal structure of the Fe-only
731 hydrogenase (CpI) from *Clostridium pasteurianum* to 1.8 angstrom resolution. *Science* **282**: 1853-
732 1858.
733 Rabus, R., Hansen, T.A., and Widdel, F., (2013) Dssimilatory sulfate- and sulfur-reducing prokaryotes. In: The
734 Prokaryotes. E. Rosenberg, E.F. DeLong, S. Lory, E. Stackebrandt & F. Thompson (eds). Berlin:
735 Springer, pp. 309-404.
736 Radianingtyas, H., and Wright, P.C. (2003) Alcohol dehydrogenases from thermophilic and
737 hyperthermophilic archaea and bacteria. *FEMS microbiology reviews* **27**: 593-616.
738 Ramos, A.R., Grein, F., Oliveira, G.P., Venceslau, S.S., Keller, K.L., Wall, J.D., and Pereira, I.A. (2015) The
739 FlxABCD-HdrABC proteins correspond to a novel NADH dehydrogenase/heterodisulfide reductase
740 widespread in anaerobic bacteria and involved in ethanol metabolism in *Desulfovibrio vulgaris*
741 Hildenborough. *Environmental microbiology* **17**: 2288-2305.
742 Ravcheev, D.A., Li, X., Latif, H., Zengler, K., Leyn, S.A., Korostelev, Y.D., Kazakov, A.E., Novichkov, P.S.,
743 Osterman, A.L., and Rodionov, D.A. (2012) Transcriptional regulation of central carbon and energy
744 metabolism in bacteria by redox-responsive repressor Rex. *Journal of bacteriology* **194**: 1145-1157.
745 Reid, M.F., and Fewson, C.A. (1994) Molecular characterization of microbial alcohol dehydrogenases.
746 *Critical reviews in microbiology* **20**: 13-56.
747 Rousset, M., Dermoun, Z., Chippaux, M., and Belaich, J.P. (1991) Marker exchange mutagenesis of the hydN
748 genes in *Desulfovibrio fructosovorans*. *Molecular microbiology* **5**: 1735-1740.
749 Rousset, M., Dermoun, Z., Hatchikian, C.E., and Belaich, J.P. (1990) Cloning and sequencing of the locus
750 encoding the large and small subunit genes of the periplasmic [NiFe]hydrogenase from
751 *Desulfovibrio fructosovorans*. *Gene* **94**: 95-101.
752 Rousset, M., Montet, Y., Guigliarelli, B., Forget, N., Asso, M., Bertrand, P., Fontecilla-Camps, J.C., and
753 Hatchikian, E.C. (1998) [3Fe-4S] to [4Fe-4S] cluster conversion in *Desulfovibrio fructosovorans* [NiFe]
754 hydrogenase by site-directed mutagenesis. *Proceedings of the National Academy of Sciences of the*
755 *United States of America* **95**: 11625-11630.

Sander, K., Chung, D., Hyatt, D., Westpheling, J., Klingeman, D.M., Rodriguez, M., Jr., Engle, N.L., Tschaplinski, T.J., Davison, B.H., and Brown, S.D. (2019) Rex in *Caldicellulosiruptor bescii*: Novel regulon members and its effect on the production of ethanol and overflow metabolites. *MicrobiologyOpen* **8**: e00639.

Schägger, H., Cramer, W.A., and von Jagow, G. (1994) Analysis of molecular masses and oligomeric states of protein complexes by blue native electrophoresis and isolation of membrane protein complexes by two-dimensional native electrophoresis. *Analytical biochemistry* **217**: 220-230.

Schägger, H., and von Jagow, G. (1991) Blue native electrophoresis for isolation of membrane protein complexes in enzymatically active form. *Analytical biochemistry* **199**: 223-231.

Schneider, C.A., Rasband, W.S., and Eliceiri, K.W. (2012) NIH Image to ImageJ: 25 years of image analysis. *Nature methods* **9**: 671-675.

Schuchmann, K., and Müller, V. (2012) A bacterial electron-bifurcating hydrogenase. *The Journal of biological chemistry* **287**: 31165-31171.

Schut, G.J., and Adams, M.W. (2009) The iron-hydrogenase of *Thermotoga maritima* utilizes ferredoxin and NADH synergistically: a new perspective on anaerobic hydrogen production. *Journal of bacteriology* **191**: 4451-4457.

Shaw, A.J., Hogsett, D.A., and Lynd, L.R. (2009) Identification of the [FeFe]-hydrogenase responsible for hydrogen generation in *Thermoanaerobacterium saccharolyticum* and demonstration of increased ethanol yield via hydrogenase knockout. *Journal of bacteriology* **191**: 6457-6464.

Sim, M.S., Wang, D.T., Zane, G.M., Wall, J.D., Bosak, T., and Ono, S. (2013) Fractionation of sulfur isotopes by *Desulfovibrio vulgaris* mutants lacking hydrogenases or type I tetraheme cytochrome c_3. *Frontiers in microbiology* **4**: 171.

Soboh, B., Linder, D., and Hedderich, R. (2004) A multisubunit membrane-bound [NiFe] hydrogenase and an NADH-dependent Fe-only hydrogenase in the fermenting bacterium *Thermoanaerobacter tengcongensis*. *Microbiology* **150**: 2451-2463.

Stolyar, S., Van Dien, S., Hillesland, K.L., Pinel, N., Lie, T.J., Leigh, J.A., and Stahl, D.A. (2007) Metabolic modeling of a mutualistic microbial community. *Molecular systems biology* **3**: 92.

Thauer, R.K., Stackebrandt, E., and Hamilton, W.A., (2007) Energy metabolism and phylogenetic diversity of sulphate-reducing bacteria. In: Sulphate-reducing Bacteria Environmental and Engineered Systems. L.L. Barton & W.A. Hamilton (eds). New York: Cambridge University Press, pp. 1-37.

Traore, A.S., Hatchikian, C.E., Belaich, J.P., and Le Gall, J. (1981) Microcalorimetric studies of the growth of sulfate-reducing bacteria: energetics of *Desulfovibrio vulgaris* growth. *Journal of bacteriology* **145**: 191-199.

Vignais, P.M., and Billoud, B. (2007) Occurrence, classification, and biological function of hydrogenases: an overview. *Chem Rev* **107**: 4206-4272.

Vignais, P.M., Billoud, B., and Meyer, J. (2001) Classification and phylogeny of hydrogenases. *FEMS microbiology reviews* **25**: 455-501.

Volbeda, A., Charon, M.H., Piras, C., Hatchikian, E.C., Frey, M., and Fontecilla-Camps, J.C. (1995) Crystal structure of the nickel-iron hydrogenase from *Desulfovibrio gigas*. *Nature* **373**: 580-587.

Wang, S., Huang, H., Kahnt, J., and Thauer, R.K. (2013) A reversible electron-bifurcating ferredoxin- and NAD-dependent [FeFe]-hydrogenase (HydABC) in *Moorella thermoacetica*. *Journal of bacteriology* **195**: 1267-1275.

Zheng, Y., Kahnt, J., Kwon, I.H., Mackie, R.I., and Thauer, R.K. (2014) Hydrogen formation and its regulation in Ruminococcus albus: involvement of an electron-bifurcating [FeFe]-hydrogenase, of a non-electron-bifurcating [FeFe]-hydrogenase, and of a putative hydrogen-sensing [FeFe]-hydrogenase. *Journal of bacteriology* **196**: 3840-3852.

Figure 1

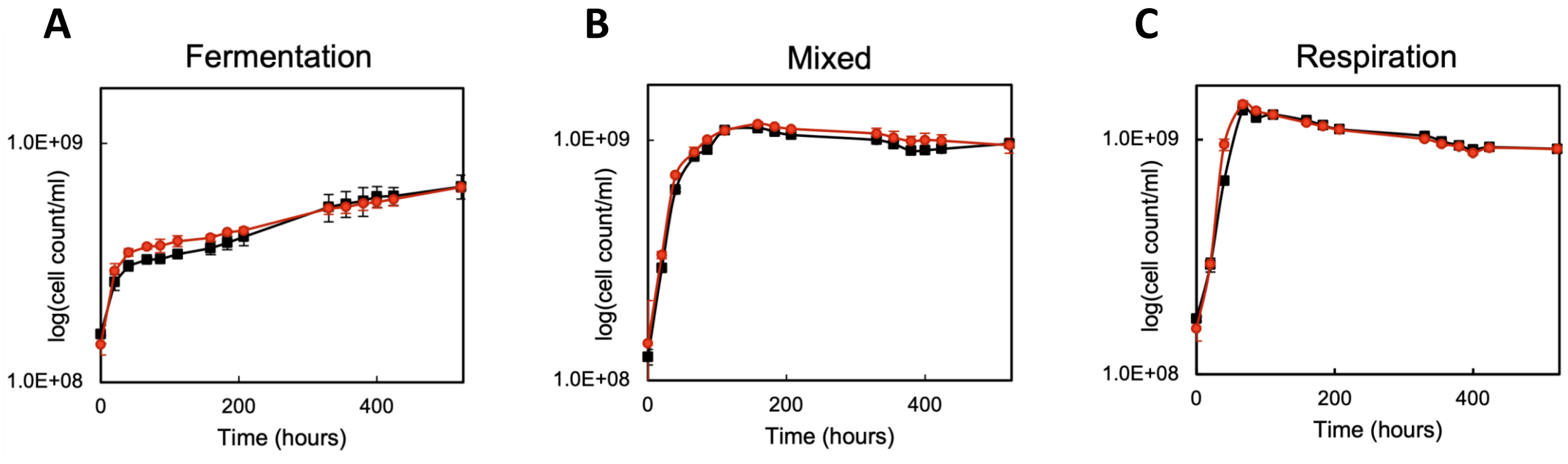
A
Fermentation
1.0E+09
1.0E+08
log(cell count/ml)
0
200
400
Time (hours)
B
Mixed
1.0E+09
1.0E+08
log(cell count/ml)
0
200
400
Time (hours)
C
Respiration
1.0E+09
1.0E+08
log(cell count/ml)
0
200
400
Time (hours)

Figure 2

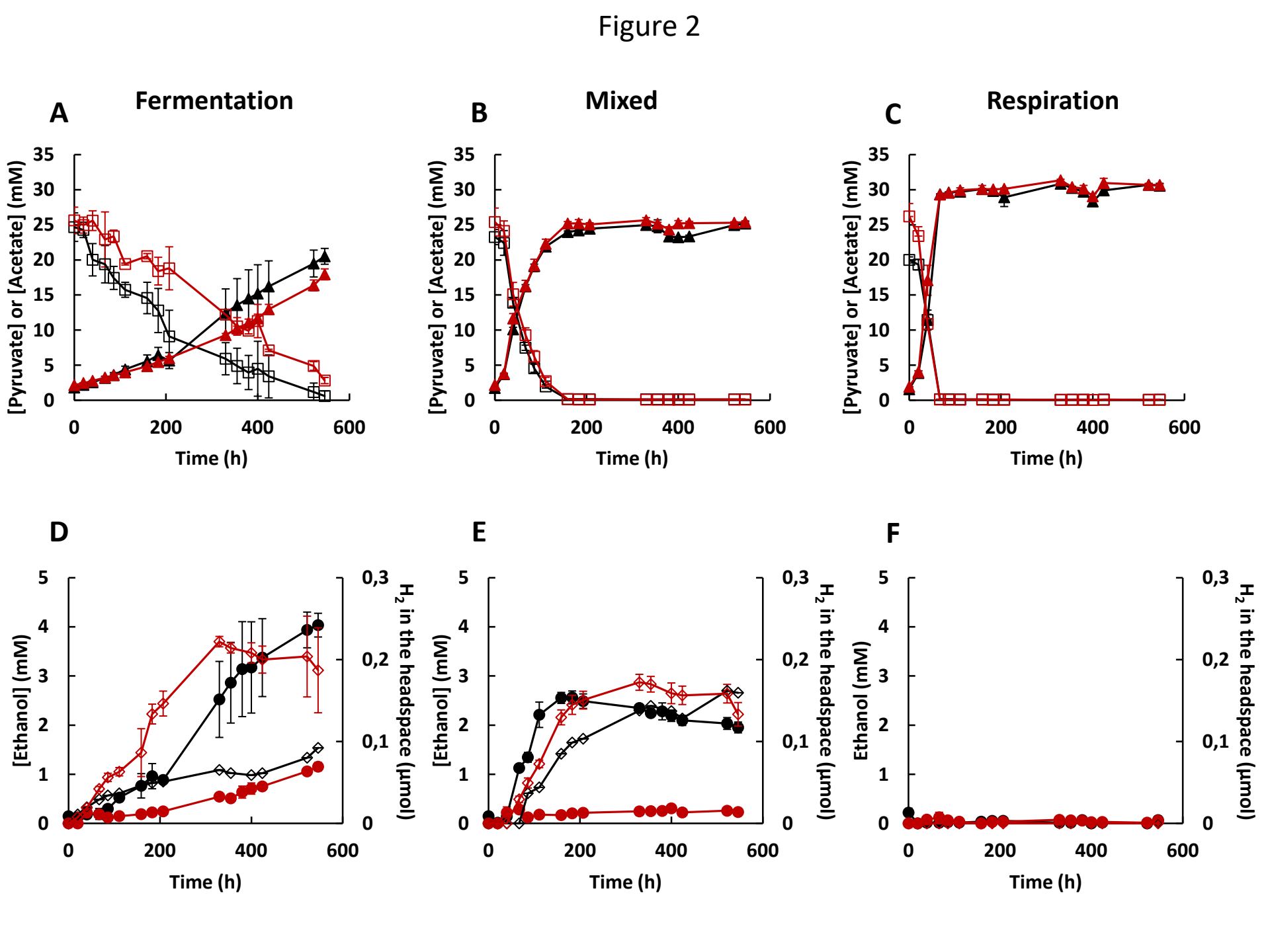
A
Fermentation
B
Mixed
C
Respiration
[Pyruvate] or [Acetate] (mM)
Time (h)
D
E
F
[Ethanol] (mM)
Ethanol (mM)
H2 in the headspace (µmol)

Figure 3

A

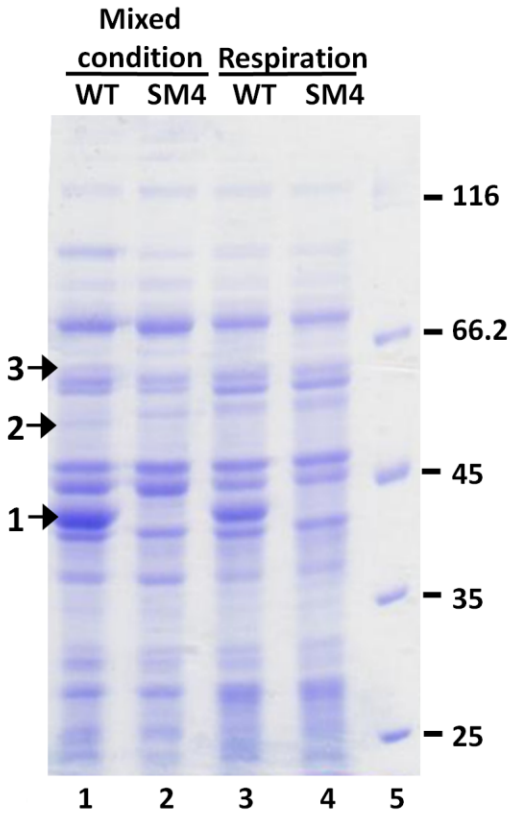

B

Band	Protein name	NCBI entry (locustag)	Unique peptides	Sequence coverage (%)	Molecular weight (kDa)
1	Iron-containing alcohol dehydrogenase	EFL49342 (DesfrDRAFT_3929)	24	41.9	41.8
2	HndC	EFL52770 (DesfrDRAFT_0400)	16	26	52.5
3	Aldehyde ferredoxin oxidoreductase	EFL50726 (DesfrDRAFT_2487)	22	43.1	60.8

Figure 4

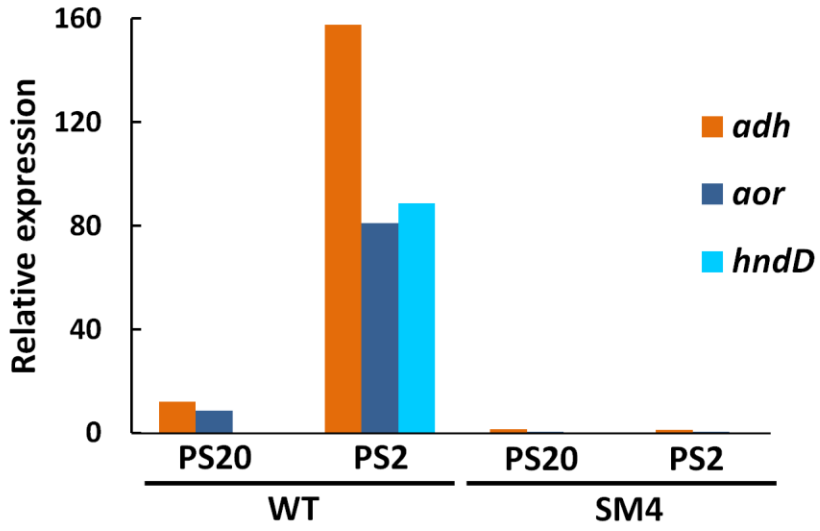
160
120
80
40
0
Relative expression
adh
aor
hndD
PS20
PS2
PS20
PS2
WT
SM4

Figure 5

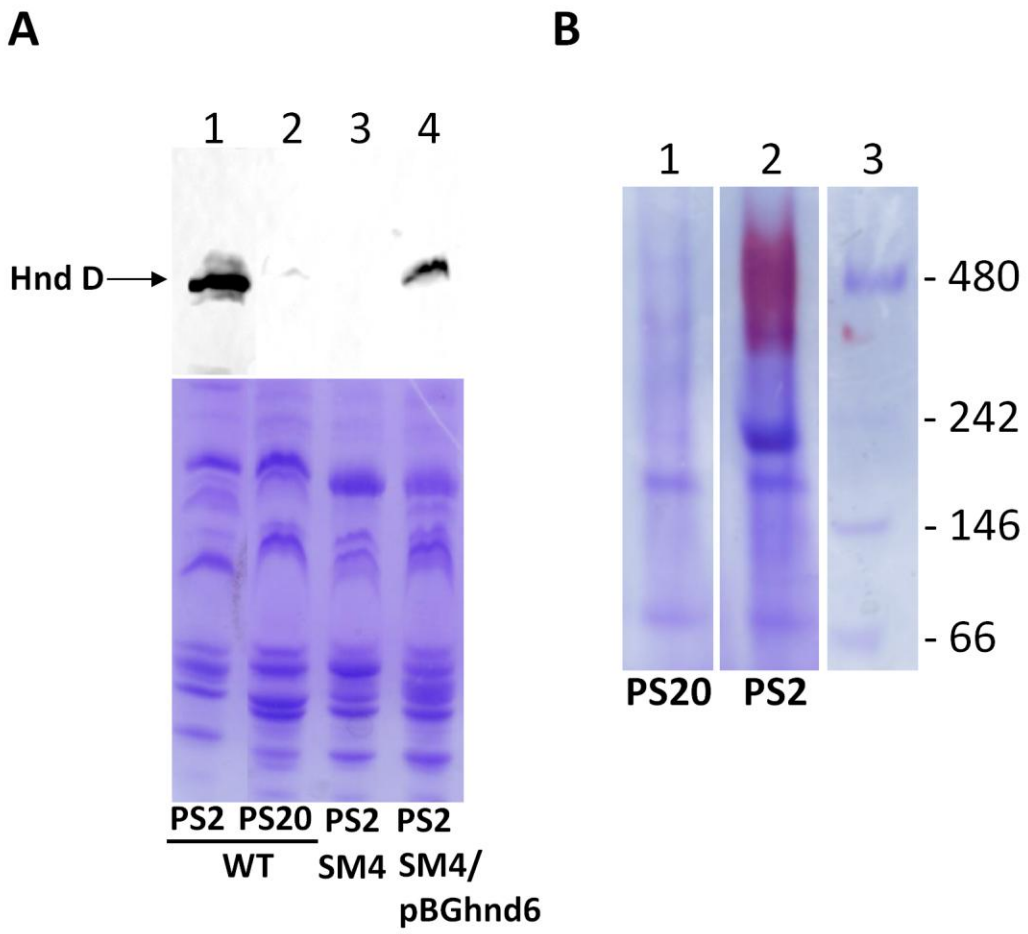
A
1 2 3 4
Hnd D
PS2 PS20 PS2 PS2
WT SM4 SM4/
pBGhnd6
B
1 2 3
- 480
- 242
- 146
- 66
PS20 PS2

Figure 6

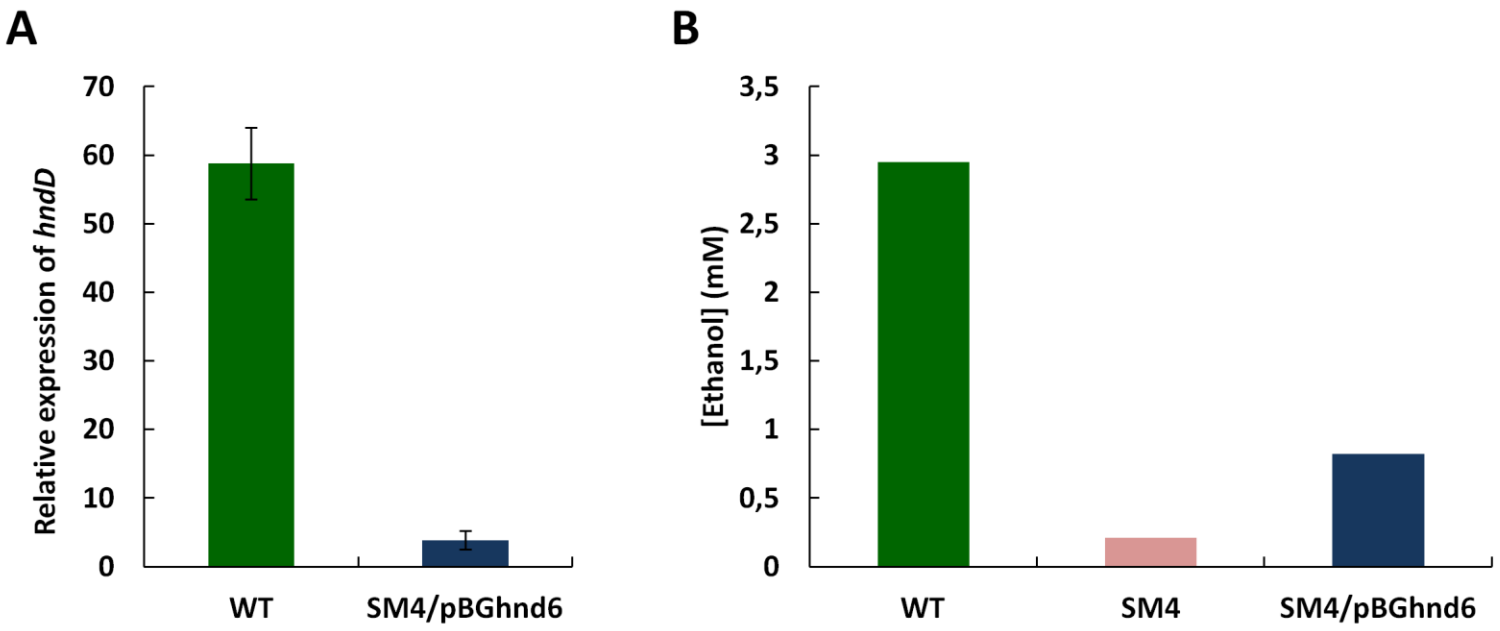
A
Relative expression of hndD
70
60
50
40
30
20
10
0
WT
SM4/pBGhnd6
B
[Ethanol] (mM)
3,5
3
2,5
2
1,5
1
0,5
0
WT
SM4
SM4/pBGhnd6

Figure 7

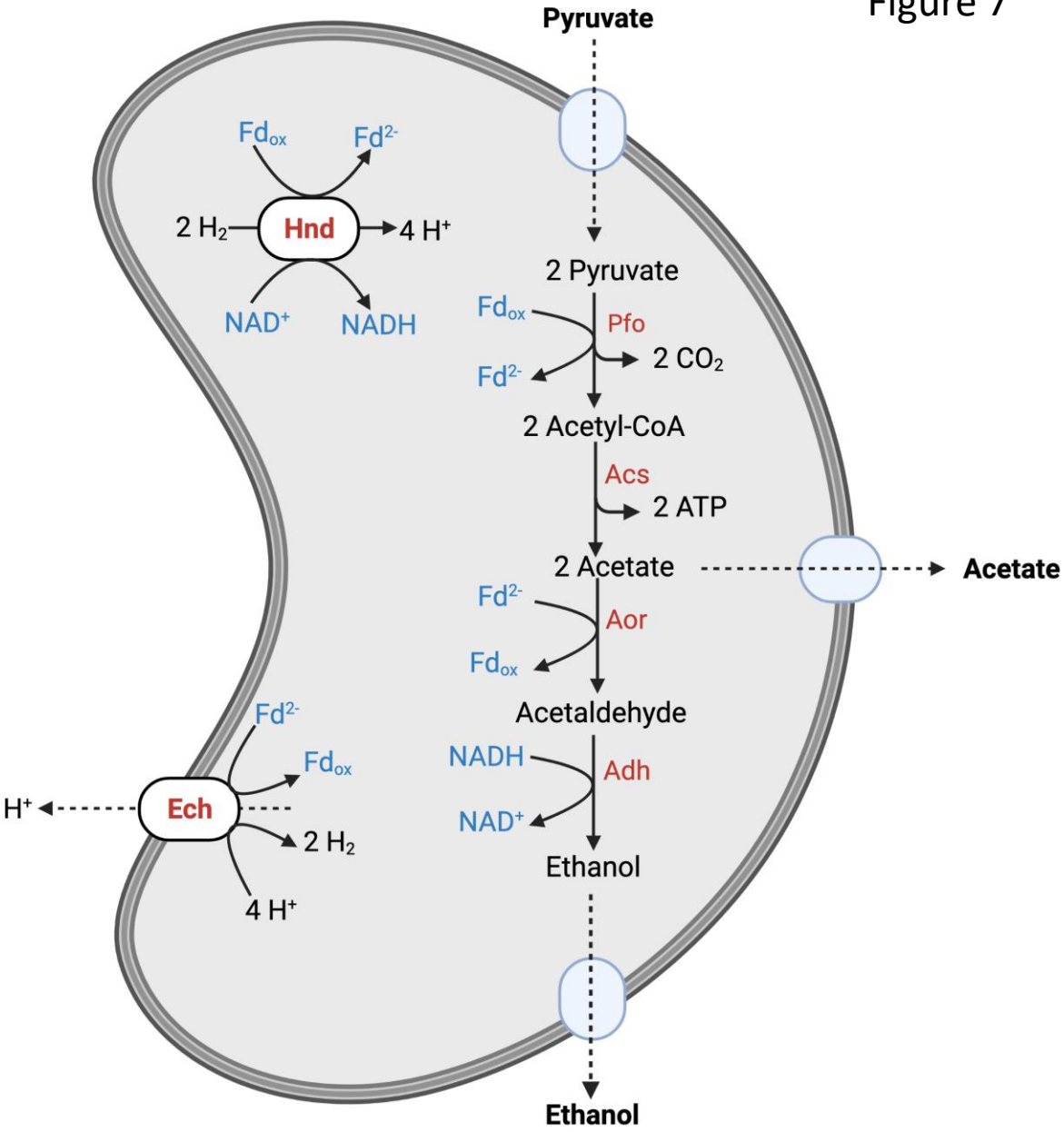
Pyruvate
Fdox
Fd2-
2 H2
Hnd
4 H+
NAD+
NADH
2 Pyruvate
Fdox
Pfo
Fd2-
2 CO2
2 Acetyl-CoA
Acs
2 ATP
2 Acetate
Acetate
Fd2-
Aor
Fdox
Acetaldehyde
NADH
Adh
NAD+
Ethanol
Fd2-
Fdox
H+
Ech
2 H2
4 H+
Ethanol

Supplementary information

The electron-bifurcating FeFe-hydrogenase Hnd is involved in ethanol metabolism in *Desulfovibrio fructosovorans* grown on pyruvate

Natalie Payne[+1], Arlette Kpebe[+1], Chloé Guendon[1], Carole Baffert[1], Julien Ros[1], Régine Lebrun[2], Yann Denis[3], Laetitia Shintu[4] and Myriam Brugna[1]*

[1]CNRS, Aix Marseille Univ, BIP, Marseille, France

[2]CNRS, Aix Marseille Univ, Plate-forme Protéomique de l'IMM, FR 3479, Marseille Protéomique (MaP), Marseille, France

[3]CNRS, Aix Marseille Univ, Plate-forme Transcriptomique, Marseille, France

[4]CNRS, Aix Marseille Univ, Centrale Marseille, ISM2, Marseille, France

[+]N. Payne and A. Kpebe should be considered joint first author

*Corresponding author: Myriam Brugna, Laboratoire de Bioénergétique et Ingénierie des Protéines, CNRS, 31 Chemin Joseph Aiguier, 13402, Marseille Cedex 20, France. mbrugna@imm.cnrs.fr

+33 4 91 16 45 68

Orcid ID Myriam Brugna: 0000-0002-4017-3294

Running title: Role of the electron-bifurcating hydrogenase Hnd

Keywords: Hydrogenase, Electron bifurcation, *Desulfovibrio*, Alcohol dehydrogenase, Aldehyde ferredoxin oxidoreductase, Ethanol

Figure S1

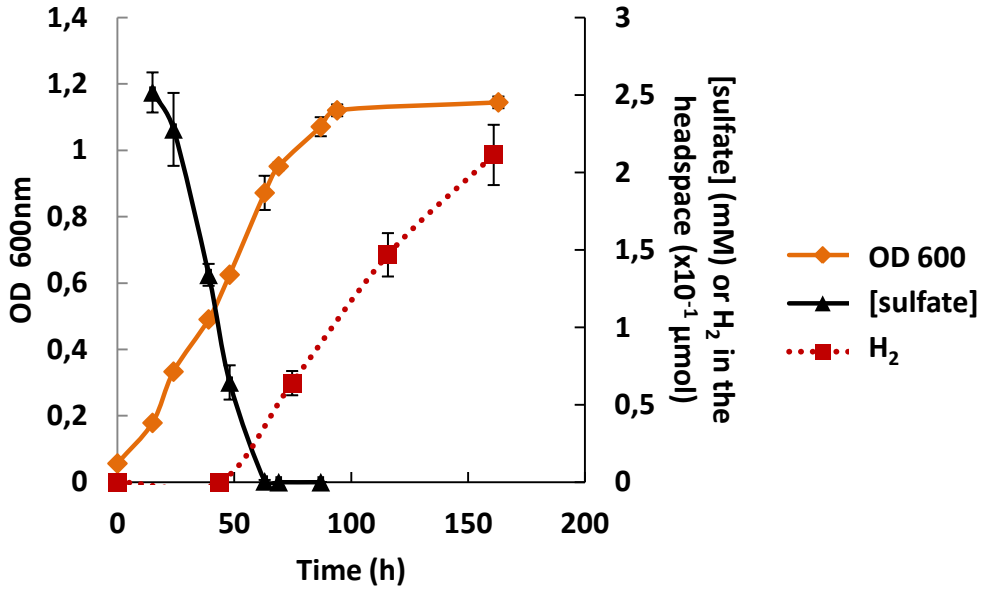

Figure S1: Growth curve, sulfate consumption and H_2 production by *D. fructosovorans* WT cells. Bacteria were grown in PS2 medium (mixed culture condition). Sulfate concentration in the growth medium was determined using a turbidimetric method with barium chloride. H_2 in the headspace was quantified using GC. H_2 starts to accumulate when sulfate is completely reduced.

Figure S2

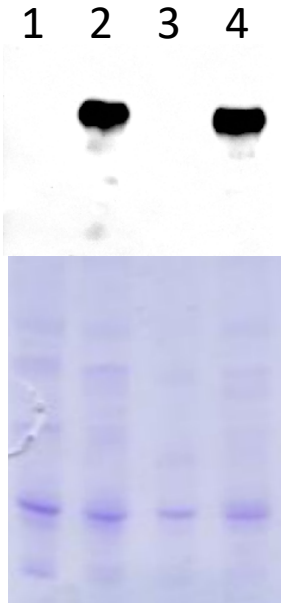

Figure S2: Western blot analysis of HndD production by *D. fructosovorans* WT cells grown in medium containing 25 mM pyruvate and 20 mM thiosulfate (lane 1), 2 mM thiosulfate (lane 2), 40 mM fumarate (lane 3) or 4 mM fumarate (lane 4) as electron acceptor. Cells were harvested at late exponential phase of growth and 2 µg of total proteins from whole-cell protein extracts were separated by 10% SDS-PAGE and subjected to western blotting using an antibody raised against HndD. The SDS-PAGE gel below the western blot is a loading control.

Figure S3

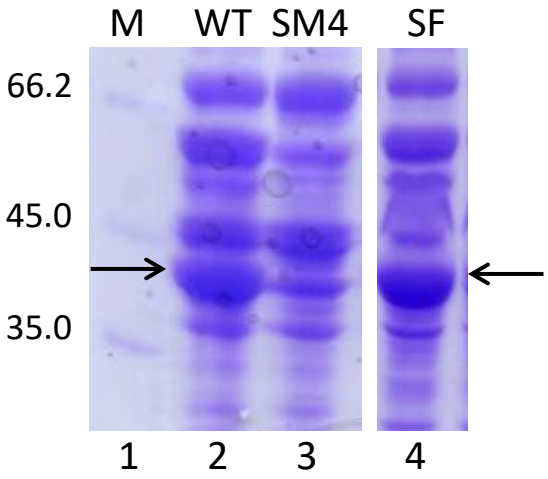

Figure S3: Separation by Coomassie-blue-stained SDS-PAGE of soluble proteins from WT (lane 2), SM4 mutant (lane 3) and SF mutant (lane 4) strains of *Desulfovibrio fructosovoran*s grown under mixed conditions (PS2). Cells were harvested at the end of the exponential phase. 45 µg of soluble proteins were loaded in each lane of a 10 % SDS-PAGE. Molecular mass markers (lane 1) are indicated in kDa. Arrows indicate bands corresponding to Adh (3929).

Figure S4

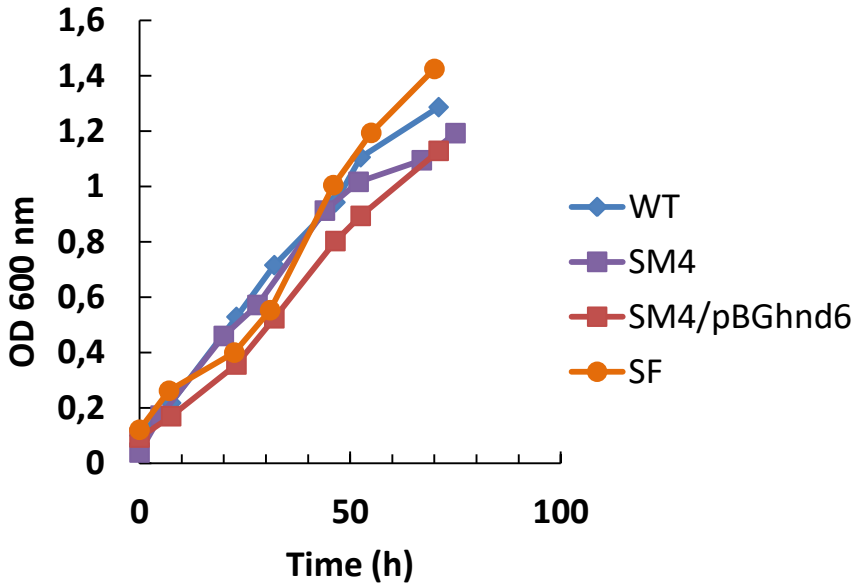

Figure S4: Growth curves of *Desulfovibrio fructosovorans* WT, SM4 (Δ*hndD*), SM4/pBGhnd6 and SF (Δ*hydAB*) strains. Bacteria were grown in PS2 medium containing 25 mM pyruvate as electron donor and 2 mM sulfate as electron acceptor (mixed culture condition).

A

B

5′-WTTGTGAWAWTWWTCACAAW-3′

C

Strain	Gene or locus tag	Rex binding site	Location
Desulfovibrio fructosovorans JJ	hndA	ATTGTGAAAATAATCACAAT	… 124 bp ATG
Desulfovibrio magneticus RS-1	hycA	TTTGTGAAAATAATCACAAA	…113 bp ATG
Desulfovibrio alcoholivorans DSM 5433	Q368_RS0118580	ATTGTGATATTTTTCACAAA	… 113 bp ATG
Desulfovibrio carbinolicus DSM 3852	C3Y92_RS00830	TTTGTGAAAATAATCACAAA	… 113 bp ATG
Desulfovibrio magneticus Maddingley MBC34	B193_3278	TTTGTGAAAATAATCACAAA	… 167 bp ATG
Desulfovibrio aerotolerans DSM 16695	GTA51_RS06440	TTTGTGAAATTAATCACAAA	… 131 bp ATG
Desulfovibrio carbinoliphilus subsp. *Oakridgensis* FW-101-B	DFW101_RS12940	ATTGTGAAAATAATCACAAA	… 131 bp ATG
Desulfovibrio sp. DV	DVDV_3691	TTTGTGAAAATAATCACAAA	… 168 bp ATG
Desulfovibrio sp. TomC	NY78_RS07160	TTTGTGAAAATAATCACAAA	… 133 bp ATG
Desulfovibrio sp. U5L	DESU5LDRAFT_RS02850	ATTGTGAAATTAATCACAAA	… 131 bp ATG

Figure S5: Predicted Rex binding-site in the promoter region of *hnd*. (A) Sequence logo of the DNA recognition motif for all Rex sites in the order Desulfovibrionales. The sequence logo was constructed based on the alignment of 117 sites identified as Rex recognition sequences (available in the RegPrecise database). (B) Consensus sequence of the Rex binding sites in the promoter region of the tetrameric, cytoplasmic [FeFe] hydrogenases found in *Desulfovibrio.* The consensus sequence was constructed by aligning the known sites with ClustalW multiple alignment. (C) The Rex binding sites and their locations in the promoter region of the tetrameric, cytoplasmic [FeFe] hydrogenases in *Desulfovibrio* species. The promoter region sequences were taken from NCBI and the Rex-binding site was mapped. Identical residues between the species are highlighted in red.

Table S1: Complete list of identified proteins of SDS-PAGE by mass spectrometry (ion trap MS/MS)

Band	Protein name	NCBI entry (locustag)	Unique peptides	Sequence coverage (%)	Molecular weight (kDa)
1	Iron-containing alcohol dehydrogenase	EFL49342 (DesfrDRAFT_3929)	24	41.9	41.8
2	HndC	EFL52770 (DesfrDRAFT_0400)	16	26	52.5
	Rhodanese domain protein	EFL49797 (DesfrDRAFT_3433)	7	18.3	48.9
	Chaperonin GroEL	EFL50342 (DesfrDRAFT_2908)	5	12.1	57.9
	Mannose-1-phosphate guanylyltransferase/mannose-6-phosphate isomerase	EFL49562 (DesfrDRAFT_3697)	5	13.4	52.6
	3-phosphoshikimate 1-carboxyvinyltransferase	EFL50559 (DesfrDRAFT_2674)	5	14.8	46.2
	Glycine dehydrogenase	EFL50313 (DesfrDRAFT_3003)	4	12.11	52.1
	[FeFe] hydrogenase H-cluster radical SAM maturase HydG	EFL51804 (DesfrDRAFT_1339)	4	10.9	53.5
	Aldehyde dehydrogenase	EFL52913 (DesfrDRAFT_0543)	3	5.3	53.1
	GHMP kinase	EFL50649 (DesfrDRAFT_2590)	2	6.5	55.9
3	Aldehyde ferredoxin oxidoreductase	EFL50726 (DesfrDRAFT_2487)	22	43.1	60.8
	Indolepyruvate ferredoxin oxidoreductase alpha subunit	EFL51374 (DesfrDRAFT_1813)	6	9.2	64.9
	Chaperonin GroEL	EFL50342 (DesfrDRAFT_2908)	5	8.2	57.9
	HndD	EFL52771 (DesfrDRAFT_0401)	4	6.8	63,4

Data correspond to identified proteins in bands 1, 2 and 3 from SDS-PAGE from WT cells grown under mixed condition (Figure 3, panel A, lane 1). Table heading: Protein name, protein name in NCBI database. NCBI entry, accession number. Unique peptides: number of distinct peptides matching to protein sequence and unique to this protein. Sequence coverage, protein sequence coverage by the matching peptides (in %). Molecular weight, theoretical molecular weight in kDa of the identified protein.

Table S2: Hydrogenase activity in the WT and the SM4 mutant strain

	Hydrogenase activity	
***D. fructosovorans* strain**	**H_2-oxidation (U/mg)**	**H_2-production (U/mg)**
WT	32.7 ± 2.5	6,4 ± 0.4
SM4	1.8 ± 0.1	0.1 ± 0.05

H_2-production and H_2-oxidation activities were measured on the soluble total extract of the 2 strains grown in mixed culture condition (PS2).

Table S3: Primers used for the PCR and RTq-PCR.

Primer	**Sequence 5'- 3'**	**Size of amplicon (bp)**
Aor-F	CTGCCCACCAAAAACTTCCG	149
Aor-R	TTATAGTGCTGGGAGCAGCG	
AdH-F	AATGACCCGCTTCTGCATCA	280
AdH-R	TTCCATGTCCTGACCGTTGG	
HND D-F	ACGTCTTCGACACCGACTTC	150
HND D-R	TCGAAGAACTTGACCCAGCC	
16S-F	GCTACGATGGGTAGCTGGTC	145
16S-R	AAGCCTTCTTCCCTCACACG	